Journal of Experimental Psychology:
Human Perception and Performance
1993, Vol. 19, No. 2, 397-415

0096-1523/93/$3.00

Coupling Dynamics in Interlimb Coordination

R. C. Schmidt, B. K. Shaw, and M. T. Turvey

In 1:1 frequency locking, the interlimb phase difference Φ is an order parameter quantifying the spatial–temporal organization of 2 rhythmic subsystems. Dynamical modeling and experimental analyses indicate that an intentional parameter Φ_ψ (intended coordination mode, $\Phi = 0°$ or $\Phi = 180°$) and 2 control parameters ω_c (coupled frequency) and $\Delta\omega$ (difference between uncoupled eigenfrequencies) affect Φ. An experiment was conducted on 1:1 frequency locking in which Φ_ψ, ω_c, and $\Delta\omega$ were manipulated using a paradigm in which a person swings hand-held pendulums. As $\Delta\omega$ deviated from 0, the observed Φ deviated from the Φ_ψ, indicating a displacement in the Φ attractor point. The displacements were exaggerated by increasing ω_c. The displacements were coordinated with a decrease in the stability of Φ and with higher harmonics in power spectrum of Φ. Implications of the results for modeling interlimb coordination are discussed.

Of general interest to the psychologist is how an animal or person can effortlessly coordinate their limbs in order to produce goal-directed actions. Everyday activity contains many complicated tasks that people perform with minimal attention and without being able to say explicitly how they perform the task. They can coordinate their lower limbs and postural system to comfortably locomote across even the most rough terrains. They can coordinate their upper limbs to reach for objects or throw them. They can coordinate their movements in synchrony with another person's in dancing or exercising. How are these often very complicated behaviors performed? What does it mean to have the knowledge for producing them?

The ecological perspective on the coordination and control of action suggests that people have tacit knowledge for producing coordinated activities in that they develop relatively autonomous control structures (i.e., coordinative structures) in the acquisition of skilled behavior that require minimal attentional intervention. It has been proposed that the autonomy of these control structures is a consequence of their being intrinsically dynamical: The functioning of these subsystems is based upon strategies of self-organization found at many scales of nature that are characterized by the components of the control structure tending toward equilibrium or steady states through mutual influence (Kugler, Kelso, & Turvey, 1980). The present manuscript reports an experiment that investigates the control structure governing a basic property of coordinated rhythmic acts, namely, the relative phasing of two rhythmic movements. In the following introductory remarks, previously proposed dynamical models of interlimb phasing are presented followed by a review of past studies that have demonstrated the dynamical nature of the control structure that governs interlimb phasing.

R. C. Schmidt, Tulane University and Center for the Ecological Study of Perception and Action, University of Connecticut; B. K. Shaw, Center for the Ecological Study of Perception and Action, University of Connecticut; M. T. Turvey, Center for the Ecological Study of Perception and Action, University of Connecticut, and Haskins Laboratories, New Haven, Connecticut.

This research was supported by National Science Foundation grants BNS 8811510 and BNS 9109880. B. K. Shaw was supported by a National Science Foundation Predoctoral Fellowship.

We thank Bruce Kay, Yves Guiard, Richard Rand and an anonymous reviewer for their helpful comments on an earlier version of this article. We also thank Paula Fitzpatrick for her help with the data analysis.

Correspondence concerning this article should be addressed to R. C. Schmidt, Department of Psychology, 2007 Percival Stern Hall, Tulane University, New Orleans, Louisiana 70118.

Dynamical Models of Interlimb Phasing

Studies of coordinated rhythmic movements have demonstrated that the relative phase angle (Φ) between two oscillating limbs is a perspicuous variable that can be used to measure interlimb rhythmic coordination (Haken, Kelso, & Bunz, 1985; Kelso, 1984; Turvey, Rosenblum, Schmidt, & Kugler, 1986). Technically, this coordination measure can be considered an *order parameter* in that (a) it captures the spatio-temporal organization of the component subsystems, and (b) it changes more slowly than the properties that characterize the states of the component subsystems. This concept plays a major role in synergetics (Haken, 1983)—a branch of physics that studies self-organizing systems at many scales of nature. In the investigation of complex (chemical, biological, social) systems, synergetics uses scale-independent physical principles to model the qualitative changes in the macroscopic patternings of these systems, that is, in their order parameters, as they are affected by changes in other properties referred to as control parameters. In the coordination of rhythmic movements, the behavior of the coordination measure Φ has been studied under the scaling of two control parameters, specifically, the coupled frequency of oscillation ω_c (Kelso, 1989; Schmidt, Carello, & Turvey, 1990) and the difference in the eigen- or inherent frequency of the component oscillators $\Delta\omega = \omega_1 - \omega_2$ (Rosenblum & Turvey, 1988) or their ratio $\Omega = \omega_1/\omega_2$ (Schmidt, Beek, Treffner, & Turvey, 1991).

The changes in the behavior of Φ that occur under the scaling of these control parameters have been modeled dynamically. The dynamical principles that have been used in the modeling are those of coupled physical oscillators. The strategy of the modeling is as follows. Consider the equa-

tions of motion of two limit cycle oscillators that are mutually coupled,

$$\dot{x}_1 = F_1(x_1) + G_1(x_1, x_2) \quad (1)$$

and

$$\dot{x}_2 = F_2(x_2) + G_2(x_2, x_1), \quad (2)$$

where x_i are vectors of variables of any dimension for oscillator i, F_i is the limit cycle component of oscillator i, and G_i is the coupling function that bidirectionally links the two oscillators. Under the assumptions that the coupling functions G_i are "weak" and the oscillatory dynamics are simply harmonic (an important and, perhaps, erroneous assumption), the effects of the coupling over each cycle can be averaged to reduce the above set of equations to a simpler set written in terms of the oscillator's phase angles (θ_i),

$$\dot{\theta}_1 = \omega_1 + H_1(\theta_2 - \theta_1) \quad (3)$$

and

$$\dot{\theta}_2 = \omega_2 + H_2(\theta_1 - \theta_2), \quad (4)$$

where ω_i is the eigenfrequency of the oscillator and H_i is a coupling/forcing function that depends upon the difference between the component oscillators' phase angles θ_1 and θ_2. If $\theta_1 - \theta_2 = \Phi$ and we subtract Equation 4 from Equation 3, then the equation for the rate of change in Φ is

$$\dot{\Phi} = \omega_1 - \omega_2 + H_1(-\Phi) - H_2(\Phi). \quad (5)$$

The equation can be simplified further if the same coupling function $H = H_{1,2}$ is assumed isotropic (operates identically in both directions):

$$\dot{\Phi} = \Delta\omega - 2H(\Phi). \quad (6)$$

This equation represents the behavior of the relative phase Φ as a function of the difference of the eigenfrequencies $\Delta\omega$ and the coupling function H.

In the literature on coordinated rhythmic movements two candidate coupling functions H have been proposed to model the patterning of Φ with changes in the control parameters ω_c and $\Delta\omega$. Haken et al. (1985) used

$$\dot{\Phi} = \Delta\omega + a\sin(\Phi) - b\sin(2\Phi) \quad (7)$$

(assuming that $\Delta\omega = 0$) to model the changes in Φ that occur through the scaling of the control parameter ω_c in bimanual index finger coordination. Rand, Cohen, and Holmes (1988) used

$$\dot{\Phi} = \Delta\omega + k\sin(\Phi) \quad (8)$$

to model the changes in Φ that occur by scaling the control parameter $\Delta\omega$ in the neural coupling of central pattern generators. Furthermore, Schmidt et al. (1991) have used a discretized version of Equation 8 that captures the effect on one oscillator's phase angle (θ_n) of the sinusoidal forcing of another oscillator,

$$\theta_{n+1} = \theta_n + \Omega - k\sin(\theta_n). \quad (9)$$

This equation, known as a circle map, was used to explain changes observed in the spectrum of Φ with changes in a control parameter that is analogous to $\Delta\omega$, namely, the ratio of $\omega_1/\omega_2 = \Omega$. As can be seen from the above derivation, the three relative phase models have a common theoretical basis in the dynamics of coupled oscillators. In the following, a summary of the findings upon which these three models are based is presented.

Changes in Mean Φ and Variance of Φ as a Function of ω_c

A basic fact of the relative phasing of limbs is that two coordinative patterns are found most prevalently, namely, the symmetric and alternate modes.[1] In the symmetric mode, the rhythmically moving limbs are at the same place in their cycles at the same time or at $\Phi = 0°$; whereas, in the alternate mode, the limbs are at opposite places in their cycles at the same time or at $\Phi = 180°$. Another basic fact is that these two relative phase modes are differentially stable—the alternate mode is less stable than the symmetric mode (Kelso, 1984; Turvey et al., 1986). One indication of this differential stability is the fact that the alternate mode becomes less and less stable as the frequency of oscillation ω_c is increased until it can no longer be maintained and a transition occurs from the alternate to the symmetric mode of phasing (Kelso, 1984). However, an identical scaling of ω_c starting in the symmetric mode yields no breakdown.

Haken et al. (1985) modeled the above properties of relative phase using Equation 7, where $\Delta\omega = 0$. Assuming that $\dot{\Phi} = \partial V/\partial\Phi$, the integration of this equation produces a potential function ($V(\Phi)$) that has a dynamical "landscape" with stable states or point attractors at $\Phi = 0°$ and 180° (Figure 1). The state of the coordinated limb system can be represented by the position of a ball in this landscape. The positioning of the ball on any sloped part of the potential function will result in the system's "relaxation" to one of these stable points. Furthermore, Haken et al. demonstrate that the topology of this attractor landscape changes as a function of the relation of the coupling strengths a and b in Equation 7. For the initial state of the system of equal strengths ($a = b$), the two attractors are present. As the ratio of $b/a = 1$ approaches $b/a = .25$, however, the attractor well at $\Phi = 180°$ disappears and only the well at $\Phi = 0°$ remains. If the system state was initially at $\Phi = 180°$, then this state would become increasingly unstable until, upon the complete annihilation of the 180° attractor, the system's state would switch to the $\Phi = 0°$ (Figure 1). Under the condition that the magnitudes of a and b are a function of ω_c, this dynamical equation can model the switch from $\Phi = 180°$ to $\Phi = 0°$ as ω_c is scaled.[2]

[1] Zanone and Kelso (1992) have demonstrated the possibility of learning other relative phase modes, however (e.g., one at $\Phi = 90°$).

[2] It should be pointed out that the transition from alternate to symmetric mode occurs both when the subject determines or when a metronome determines the frequency of oscillation. Modeling the metronome as an external forcing function, and thus making

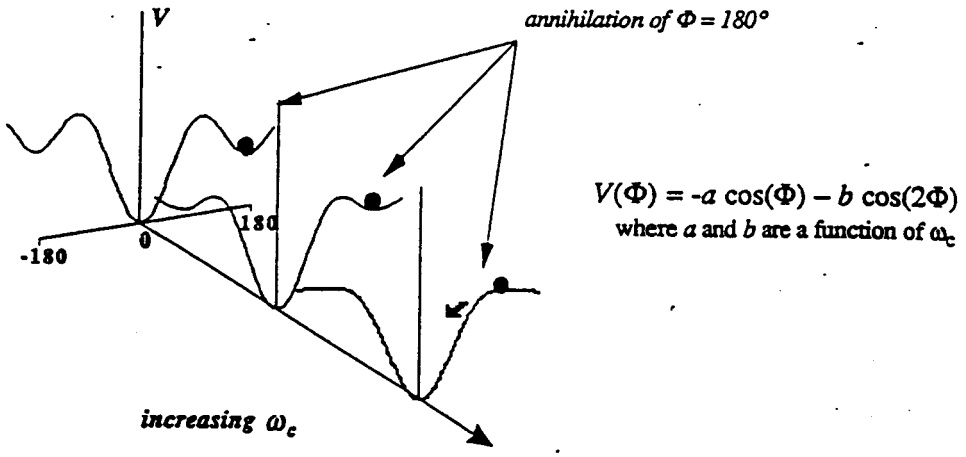

Figure 1. Haken, Kelso, and Bunz's (1985) dynamical model of the changes in the coordination variable Φ with the scaling of control parameter ω_c. (The topology of the dynamical landscape of the order parameter Φ changes as the control parameter ω_c is increased. At a critical value of ω_c, the stable point at Φ = 180° is annihilated, and a transition to relative phase angles near Φ = 0° occurs.)

This kind of nonlinear change of state that results from the scaling of a control parameter is known in physics as a bifurcation or a catastrophe (Gilmore, 1981; Haken, 1983). Much empirical work done by Kelso and colleagues has demonstrated that this nonlinear change of coordination modes indeed has the hallmark properties of a physical bifurcation: critical fluctuations (a dramatic increase in fluctuations immediately before the transition, Kelso, Scholz, & Schöner, 1986), critical slowing down (increased time to return from a perturbation, Scholz, Kelso, & Schöner, 1987), and hysteresis (decreasing the ω_c does not lead to a reverse jump back into the alternate mode after the transition to the symmetric mode had occurred, Kelso & Kay, 1987). In short, these studies have verified that the empirical properties of the breakdown in alternate interlimb phasing has properties that are predicted by Equation 7 under a scaling of the frequency of oscillation (ω_c).

Changes in Mean Φ as a Function of Δω

In a number of biological systems, if the rhythmic units involved have different inherent frequencies or eigenfrequencies, the relative phase angle Φ that is observed between the oscillation of units when coordinated at the same tempo is not perfectly at 0° or 180° (although the coordination modes intended were the symmetric and alternate modes, respectively) but some small deviation ΔΦ away from 0° and 180°. This phase lag ΔΦ is such that (a) the rhythmic unit with the slower eigenfrequency is always behind the faster unit in phase even though they have the same coupled frequency and (b) the magnitude of this phase lag is a linear function of the eigenfrequency difference (Δω). These characteristics were first observed by von Holst (1939/1973) in the coordination of fish fins. He called the phenomenon the *maintenance tendency* because he claimed that each rhythmic unit was trying to maintain its own inherent frequency and the phase lag was the result of the balancing of the "forces" of the individual oscillators. These maintenance tendency characteristics have also been observed on the neural level as well in the coordination of the CPGs in the crayfish swimmeret system (Stein, 1973, 1974).

The maintenance tendency has been primarily observed in the bimanual coordination of wrist movements in humans using a methodology known as the *wrist-pendulum paradigm* (Kugler & Turvey, 1987) in which the eigenfrequencies of the individual rhythmic units can be manipulated. In this paradigm, a subject must coordinate two hand-held pendulums with either identical or different masses and lengths in (a) a comfortable 1:1 frequency lock (i.e., at the same tempo) and (b) either the symmetric or the alternate relative phase modes. The eigenfrequency of a single wrist-pendulum system is determined as that frequency that is most comfortable for long-term oscillation and has been found to be very near the pendulum's gravitational frequency ($2\pi\omega = \sqrt{g/\text{length}}$). The eigenfrequencies can be manipulated in the wrist-pendulum paradigm because they are a function of the inertial loadings of the pendulums: The eigenfrequencies of short length and light mass wrist-pendulum systems are high and those of long length and heavy mass wrist-pendulum systems are low. The control parameter Δω can then be manipulated by having a subject swing two pendulums of different sizes (one in each hand) in a 1:1 frequency lock. As with fish fins and neural CPGs, the wrist-pendulum system with the lower eigenfrequency lags in phase and the magnitude of this ΔΦ depends upon the magnitude of the left–right imbalance (i.e., Δω) (Bingham,

the coupled autonomous oscillators nonautonomous, is not seen as necessary in the first pass of modeling this phenomenon. However, the external "forcing" of the system that is in the perceptual tuning of the control structure indeed renders the system nonautonomous in nature. How to incorporate nonautonomous dynamics nonarbitrarily into perceiving-acting systems has been discussed elsewhere (Beek, Turvey, & Schmidt, 1992).

Schmidt, Turvey, & Rosenblum, 1991; Rosenblum & Turvey, 1988; Schmidt et al., 1991; Turvey et al., 1986).

The explanations of maintenance tendency in human bimanual coordination have attempted to give credence to von Holst's "balancing of forces" idea. Rosenblum and Turvey (1988) suggest, following Partridge (1966, 1967), that the patterning of the relative phase Φ is a consequence of the general phenomenon of latencies in electromechanical response of the musculature which are inertia dependent. Same inertia wrist-pendulum systems will produce the equivalent latencies in the musculature, and hence, no deviation from intended relative phase (i.e., $\Phi = 0°$ or $\Phi = 180°$); however, different inertia wrist-pendulum systems will produce different latencies in the musculature, and hence, a deviation $\Delta\Phi$ from intended relative phase. Bingham et al. (1991) accepted this hypothesis and point out that the property that is responsible for the magnitude of muscular latency is the stiffness assembled at the wrist to move the inertial loading of the pendulum at the frequency required by the 1:1 frequency lock. The fact that the difference in the estimated stiffness assembled at the two wrists (right stiffness – left stiffness), which can be said to index the compromise of the forces at the two wrists, linearly scales the deviation $\Delta\Phi$ from intended relative phase (Bingham et al., Figure 9) supports von Holst's "balancing of forces" hypothesis.

A dynamical systems exposition of the balancing of forces hypothesis for systems under a $\Delta\omega$ parameterization is found in the neural oscillator literature but can accommodate the human bimanual oscillation data as well. In modeling the changes of Φ with $\Delta\omega$ observed such as those observed by Stein (1973, 1974), Kopell (1988) and Rand et al. (1988) proposed that the dynamical models of Φ presented in Equations 6 and 8, respectively. Kopell proposed a general model of which the Rand et al. model is a particular instantiation. Rand et al. chose the coupling function $H = k \sin(\Phi)$ because it captures the key characteristics of Φ empirically observed under $\Delta\omega$ scaling, namely, (a) an increasing phase lag with deviation of $\Delta\omega$ from 0 and (b) the two basic relative phase modes at $\Phi = 0°$ and $\Phi = 180°$.

These two characteristics can be demonstrated in terms of the properties of a potential function V that represents the attractor layout for this system. Given that the coupling strength k is large with respect to $\Delta\omega$, the attractor layout for Equation 8 has a single well, and hence, a single stable state or point attractor (as compared to that of Equation 7 in Figure 1). Equation 8 has the characteristic that, assuming a constant k, the position of the attractor's stable point is a function of $\Delta\omega$ (Figure 2). In particular, a deviation in $\Delta\omega$ from 0 causes the location of the stable points to move away from $\Phi = 0°$ and $\Phi = 180°$ (i.e., causes a $\Delta\Phi$). Larger deviations in $\Delta\omega$ from 0 move the location of the attractor point farther from $\Phi = 0°$ or $\Phi = 180°$. The position of the attractor's stable point is an indication of the balancing of forces of the two component oscillators.

Furthermore, although the model has only one potential well, it can model both the symmetric and alternate relative phase modes. If the strength of coupling k is positive, the stable point is near $\Phi = 0°$; if k is negative, the stable point

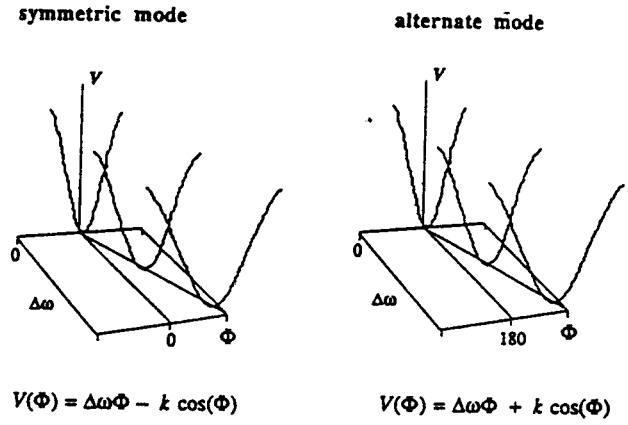

Figure 2. Rand, Cohen, and Holmes's (1988) dynamical model of the changes in the coordination variable Φ with the scaling of the control parameter $\Delta\omega$. (Deviations of the control parameter $\Delta\omega$ from 0 lead to a procession of the stable relative phase angle at the bottom of the potential well away from the intended relative phase angles at $\Phi = 0°$ and $\Phi = 180°$. The two relative phase modes are attained in this model by the sign of the coupling strength k. Note that the sign of k changes as one moves from the differential [Equation 8] to the integral form [this figure] of the model.)

is near $\Phi = 180°$. As a matter of fact, the scaling of this coupling strength can lead to the breakdown of coordinative modes modeled by Haken et al. with Equation 7: Decreasing the absolute magnitude of the coupling strength (i.e., $|k|$) will lead to increasing instability of the attractor and to a breakdown of the phase locking as k passes through a critical value that depends upon the magnitude of $\Delta\omega$ (Rand et al., 1988). Assuming (as Haken et al., 1985) that the magnitude of this coupling strength decreases with increasing frequency, Equation 8 can model the breakdown in alternate mode phasing with increasing ω_c as well. What Equation 8 fails to predict (that Equation 7 does) is the asymmetry in the breakdown in phasing—it occurs only in alternate mode. Equation 8 can accommodate this fact, however, by assuming the boundary condition that the coupling strength for alternate mode is in general weaker than that of the symmetric mode. It should also be noted that Equation 7, with constant coupling strengths a and b, also produces an increased deviation of its attractors' stable points with the scaling of $\Delta\omega$. With these differences noted, the two equations can be seen as alternative explanations for the changes of Φ with the scaling of ω_c and $\Delta\omega$ because each can explain the effects of both control parameters.

Changes in the Variance of Φ as a Function of $\Delta\omega$

Not only does the deviation from intended Φ increase as the control parameter $\Delta\omega$ deviates from 0, but also the variability of Φ as measured by the power of the Φ spectrum increases as $\Delta\omega$ deviates from 0. The explanation of this result can be seen in terms of the circle map representation of coupled oscillators (Equation 9). An important point, stated above, is that this representation is a discretized version of the Rand et al. Equation 8. The state map of the

circle map regime, known as an *Arnold tongues* diagram (Schmidt et al., 1991, Figure 2), represents the stable frequency locking patternings that two oscillators under a sinusoidal coupling (H) can have given a difference in eigenfrequencies (appearing in the circle map as $\Omega = \omega_1/\omega_2$) and a coupling strength k. Schmidt et al. point out that the Arnold tongue for 1:1 frequency locking becomes narrower and narrower as the eigenfrequency difference increases. This can be interpreted as indicating that the appropriate coupling strengths k, necessary for maintaining 1:1 frequency locking, get fewer and fewer in number as Ω deviates from 1 (or as $\Delta\omega$ deviates from 0). Because the number of possible coupling strength magnitudes decrease for any given Ω away from $\Omega = 1$, the fluctuations in Φ increase.

The increase in variability of Φ as $\Delta\omega$ deviates from 0 can also be explained by the continuous dynamical model found in Equation 8. In Figure 2, not only does the place of the point attractor change as $\Delta\omega$ deviates from 0 but the concavity of the potential ($d^2V/d\Phi^2$) becomes shallower. The concavity of the well is an index of the strength and *relaxation time* of the attractor, the time the system takes to return from a perturbation: The greater the concavity, the greater the relaxation time, and the greater the relaxation time, the weaker the attractor. Furthermore, assuming that the control structure assembled has a constant amount of noise from its microstructure (Schöner, Haken, & Kelso, 1986), this constant noise would manifest itself as greater fluctuations in Φ as the attractor becomes weaker.[3] This explanation furthers the circle map/Arnold tongue hypothesis by demonstrating why the Arnold tongue becomes narrower as $\Delta\omega$ deviates from 0: The attractor for the 1:1 frequency lock patterning becomes weaker and only certain coupling strengths k can keep it from becoming completely unstable.

Scaling of the eigenfrequency difference $\Delta\omega$ has also been found to affect the local and global patterning of power in the Φ spectrum (Schmidt et al., 1991). First, the Φ spectrum has been found to be composed of peaks at integer multiples of the oscillation frequency (i.e., a harmonic organization of the power). This local patterning of power signifies that there are rhythmicities latent in the variability of Φ. Furthermore, it was found that the general increase in total power with deviations from $\Delta\omega = 0$ was due only to the increases of power at the peaks: The peaks became taller as the control parameter $\Delta\omega$ was scaled and new peaks emerged.

The spectral peaks of the Φ spectrum have been interpreted as representing control processes that are harnessed to deal with the ensuing instability of the dynamical regime assemble to govern the coordination (e.g., Equation 8). What this hypothesis proposes is that (a) appropriating a dynamical regime to control coordination has its costs because instability occurs under different parameterizations and (b) additional control processes have to be brought to bear in order to keep the control structure stable. If the spectral peaks in the relative phase spectrum are taken to be an index of these control processes, it can be said that growing instability is "packaged" by these control processes at the time scales of the spectral peaks. Schmidt et al. (1991) suggested that the control processes that are subsidiary to the main dynamical regime are processes of perceptual tuning. In particular, the peaks may represent control points at which information about the coordination is picked up (Beek, 1989). Hence, an increase in the number of peaks could indicate an increase in information pickup (see the General Discussion section).

The fact that there is coherent patterning of the Φ variance in the form of rhythmicities indicates that the interlimb phasing of the coupled wrist-pendulum systems is not one of phase locking but rather phase entrainment: The phase angles of the two oscillators are attracted to one another but not perfectly locked (Keith & Rand, 1984). The distinction between the two kinds of coordination is elucidated in Figure 3 (upper panel). The importance of this point is that the dynamical models so far presented account for phase locking behavior only, not phase entrainment; Equation 8 would predict a general increase in total power with deviation of $\Delta\omega$ from 0 but not coherently packaged power at harmonically related spectral frequencies. How is this phase entrainment pattern to be explained? Two explanation are possible. The phase entrainment pattern can be explained by (a) incorporating other processes besides those of Equation 8 into the architecture of the coupling function (H_i) underlying the coordination or by (b) making the oscillatory dynamics (the F_i in Equations 1 and 2) not simply harmonic but nonlinear counter to the assumptions of the averaging procedure of Rand et al. (1988). Refinement of the models along these lines is explored in the discussion.

The Φ spectrum not only has a local patterning of the Φ power in the form of spectral peaks but has also a global patterning that has a $1/f^{\delta}$ topology (Figure 3, lower panel). These spectra are called *inverse power-law spectra* (West & Shlesinger, 1990). Such spectra have been observed in complex systems such as biological organisms (Goldberger, Bhargava, West, & Mandell, 1985; Goldberger, Kobalter, & Bhargava, 1986; Koboyashi & Musha, 1982; Musha, Katsurai, & Teramachi, 1985) that function on multiple space–time scales. The topology of their spectra indicates a relation between the amounts of power (or energy) that occur at different time scales, namely, the magnitude of power is a function of the inverse of the frequency (i.e., period) of the subtask. Systems that have these interrelationship of subtasks have a *fractal* or scale-invariant organization (West & Shlesinger, 1989).

The δ of the $1/f^{\delta}$ scaling is indicative of the amount of correlation between the subtasks of a system. A $\delta = 0$ (a white-noise process) would indicate no correlation between subtasks. But as δ increases from 0, there is an increasing amount of correlation between the subtasks because more power will be concentrated in one particular part of the spectrum (the lower frequencies). Schmidt et al. (1991) found that the δ magnitudes of the Φ spectra were scaled by the left–right imbalance of the coupled wrist-pendulum sys-

[3] Essentially, a noise perturbation with given magnitude of force F will travel farther up the potential well when the slope of the well is less steep.

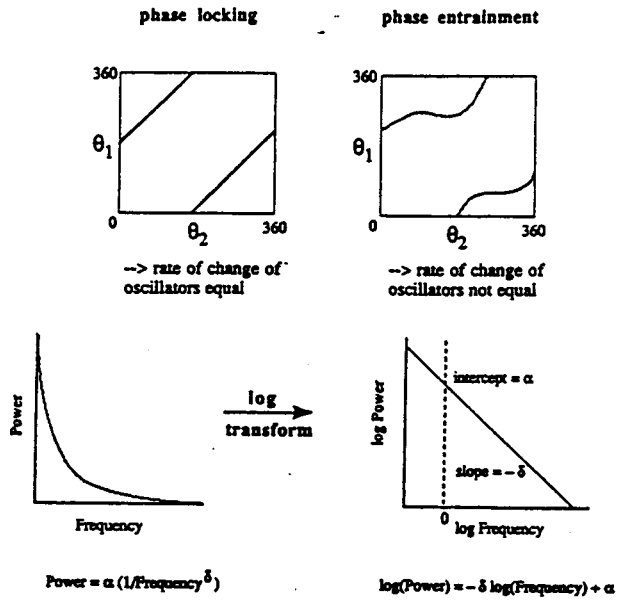

Figure 3. The top panel shows the difference between oscillators that are phase locked and phase entrained (after Keith & Rand, 1984). (When two oscillators are phase locked, a phase–phase plot has a constant slope. When two oscillators are phase entrained, their phase–phase plot has a changing slope.) The lower panel demonstrates a $1/f$ power spectrum. (These have a hyperbolic distribution of power across the frequency range, power = $\alpha\ 1/f^{\delta}$, which upon a transformation to logarithmic coordinates becomes linear, log(power) = $-\delta \log(f) + \alpha$.)

tems as indexed by the control parameter $\Omega = \omega_1/\omega_2$. At $\Omega = 1$, δ had magnitudes near 2. But as Ω decreased to values far from 1, δ approached magnitudes near 1, suggesting that the correlations between the subtasks decreased as the eigenfrequencies of the component oscillators became more different. This decreased correlation was interpreted as an accommodation to the increasing internal perturbations caused by the narrowing of the 1:1 frequency lock region (Arnold tongue) of the regime's state space.

Simultaneous Manipulation of ω_c and $\Delta\omega$

In the present study, we investigated the coordination of two moving limbs as indexed by the order parameter Φ under the simultaneous scaling of the two control parameters, ω_c and $\Delta\omega$. Furthermore, these manipulations were carried out in the intended (Ψ) coordination modes of $\Phi_\Psi = 0°$ and $\Phi_\Psi = 180°$. Of general interest is how the patterning of Φ previously observed for the manipulation of $\Delta\omega$ is affected by different frequencies of oscillation ω_c, and whether the effects of these two control parameters is the same for the symmetric and alternate modes of coordination. Of specific interest is how well the candidate dynamical models (Equations 7–9) based on 2π-periodic coupling functions address the pattern of dependencies of Φ on Φ_Ψ, ω_c, and $\Delta\omega$.

The simultaneous effect of the two control parameters, ω_c and $\Delta\omega$, on the two coordination modes has not heretofore been observed. These control parameters have been previously investigated only in different studies with different effector systems only. Kelso and colleagues (Kelso, 1984, 1989; Kelso et al., 1986) have extensively investigated the effect of ω_c on interlimb phasing using the bimanual oscillation of index fingers. Turvey and colleagues have extensively investigated the effect of $\Delta\omega$ on interlimb phasing using the bimanual oscillation of hand-held pendulums swung from the wrist. The present study examines the simultaneous effect of the two control parameters using the latter methodology. Furthermore, an attempt is made to explain the effects of both control parameters in terms of a single dynamical model. Previously, the effects of the two control parameters have been explained by different dynamical models, the effects of ω_c by Equation 7 and the effects of $\Delta\omega$ by Equation 9. Also, the effectiveness of the Rand et al. equation in modeling macroscopic limb movements has not been previously evaluated.

Method

Subjects

Seven subjects participated in the experiment, 2 men and 5 women. Three of the subjects were University of Connecticut graduate students, 3 were undergraduates fulfilling a course requirement, and the other was not affiliated with the University of Connecticut. Two subjects' data were discarded because their relative phase time series revealed spontaneous transitions or very large and uneven fluctuations that violated the stationarity conditions necessary to perform power spectral analysis on a time series. Therefore, 5 subjects' data were used in the analysis. All subjects were naive to the purpose of the experiment.

Materials

The pendulums were constructed using the specifications described in Kugler and Turvey (1987). They consisted of an ash dowel with a bicycle hand grip attached to the top. Mass weights were attached to a 10-cm-long bolt that was drilled through the dowel at right angles 2 cm from the bottom. Four such pendulums were used. The length and mass magnitudes were 0.31 m and 0.2 kg for Pendulum A, 0.48 m and 0.2 kg for Pendulum B, and 0.75 m and 0.2 kg for Pendulums C and D. The effective mass and length of a single wrist-pendulum system have been taken to be the equivalent simple pendulum mass and length of the compound pendulum consisting of the attached mass, the dowel and the hand of the subject. These magnitudes were calculated using the algorithm reported in Kugler and Turvey (1987). The characteristic frequencies (ω_i) of these simple equivalent pendulums considered as gravitational pendulums are displayed in Table 1.

Each subject was asked to oscillate isochronously five combinations of the pendulums during the experiment: The two longest together, the longest in the right hand with each of the two shorter ones in the left hand, and the longest in the left hand with each of the two shorter in the right hand. The design of these coupled wrist-pendulum systems along with the difference in the eigenfrequencies $\Delta\omega$ ($= \omega_{right} - \omega_{left}$) is displayed in Table 2. Note that negative $\Delta\omega$ values indicate pendulum pairs in which the left system is smaller and has a greater frequency of oscillation than the right and positive $\Delta\omega$ values indicate pendulum pairs in which the right system is smaller and has a greater frequency of oscilla-

tion than the left. Note as well that manipulating $\Delta\omega$ is tantamount to manipulating the left–right imbalance of the pendulum systems.

Subjects sat in a specially designed chair with armrests to support their forearms. The armrests were designed to restrict the subjects' swinging movements to the wrist; the forearm was kept continually resting on the arm support. The chair also raised the subjects' legs with supports so that they did not interfere with the ultrasonic acquisition of the data (see below).

Wrist-pendulum movement trajectories were collected using an UltraSonic 3-Space Digitizer (SAC Corporation, Stratford, CT). An ultrasound emitter was affixed to the end of each pendulum. An ultrasound "spark" was issued from each emitter 90 times per second. The digitizer operates by registering each emission using three microphones arranged to form a square grid. The digitizer calculates the distance of each emitter from each microphone, thereby pinpointing the position of the emitters in the three dimensions at the time of the emission. This slant range information was stored for later use on an 80286-based microcomputer using MASS digitizer software (Engineering Solutions, Columbus, Ohio). This software and analogous routines written on a Macintosh II use the slant range time series to calculate the primary angle of excursion of the pendulums and their relative phase angle Φ. An electronic metronome was used in trials in which subjects were instructed to swing the pendulums at a preset frequency.

Procedure and Design

The subjects were asked to coordinate one of the five possible pairings of pendulums in Table 2 in either the symmetric phase mode ($\Phi_\Psi = 0°$) or alternate phase mode ($\Phi_\Psi = 180°$). The subscript Ψ is used here to denote that these were the ~~relative~~ phase angles that the subject intended. The frequency of oscillation (ω_c) at which a subject coordinated the pendulums was either a self-selected comfort frequency or one of two preset frequencies, 0.93 Hz or 1.15 Hz. These frequencies were chosen because they were in the upper, or above comfort mode, frequency range observed in wrist-pendulum swinging. Frequencies in the lower frequency range (below the comfort mode) are investigated by Sternad, Turvey, and Schmidt (1992). In comfort frequency trials, the metronome was off; in the other trials, it was turned on at the preset frequency before data recording began. Thus the design of the experiment was a factorial one that consisted of two intended relative phase modes (Φ_Ψ), three kinds of frequencies (ω_c), and five coupled pendulum systems ($\Delta\omega$). Both the coordination mode and the frequency of oscillation were specified at the beginning of a trial. There was one 60-s trial per condition for a total of 30 trials per subject. The order of trials was randomized, with the constraint that the $\Phi_\Psi = 0°$ and $\Phi_\Psi = 180°$ trials for a given combination of $\Delta\omega$ and ω_c were next to each other. This constraint expedited the experimental session because the pendulums needed to be changed only every other trial rather than every trial.

Table 1
Characteristic Frequencies of the Simple Equivalent Pendulums (in Hz) Considered as Gravitational Pendulums

Subject	Pendulum A	Pendulum B	Pendulum C	Pendulum D
1	1.037	0.806	0.637	0.637
2	1.007	0.792	0.632	0.632
3	1.022	0.799	0.635	0.635
4	1.009	0.793	0.632	0.632
5	1.026	0.800	0.635	0.635

Table 2
Design of the Coupled Wrist-Pendulum Systems and the Average Value of $\Delta\omega$ (in Hz)

System	Left pendulum	Right pendulum	$\Delta\omega$
1	C	A	.386
2	C	B	.164
3	C	D	0
4	B	D	−.164
5	A	D	−.386

Each subject was given instructions and allowed to practice before the beginning of a session. He or she was told to place the forearms squarely on the arm rests, to gaze straight ahead without looking at the pendulums, and to swing the pendulums smoothly back and forth. The subject was instructed to hold the pendulums firmly in the hands so that as much of the rotation of the pendulum as possible was created about the wrist joint rather than about the finger joints. The subject was allowed to practice the task in both phase relations and all frequency conditions for a subset of the coupled pendulum system combinations. At the beginning of each trial, the subject was allowed as much time as needed to achieve the goal of the condition. Data recording began after the subject indicated that he or she was ready. Subjects were allowed to rest between the trials of a session when they needed to.

Data Reduction

The digitized displacement time series of the wrist-pendulum systems were smoothed using a triangular moving average procedure.[4] Each trial was subjected to software analyses to determine the frequency of oscillation of each wrist-pendulum system, the time series of the relative phase angle Φ between the two wrist-pendulum systems, the power spectra of this relative phase time series, and the total power associated with each of these spectra.

A peak picking algorithm was used to determine the time of maximum forward extension of the wrist-pendulum trajectories. From the peak extension times, the frequency of oscillation for the nth cycle was calculated as

$$f_n = \frac{1}{(\text{time of peak extension}_{n+1} - \text{time of peak extension}_n)}. \quad (10)$$

The mean frequency of oscillation for a trial was calculated from these ~~cycle frequencies~~. The phase angle of each wrist-pendulum

[4] Subsequent to the data collection, we realized that a number of the data records had noise in them that the moving average procedure could not efficiently smooth. The reason for this is the following. One of the perils of using a sound-based acquisition system is the reflection of previous emissions back to the microphones from hard surfaces in the experimental area. These erroneous points appear as extreme outliers and can be identified by software error checking routines. When this occurs either correct points are interpolated or, if software interpolation is not possible, the trial is repeated. Unfortunately, the error-checking routines used at the time of data collection were faulty such that trials that would have been repeated were not identified. Hence, the erroneous points were eliminated post hoc using a laborious graphical interpolation procedure in which single points were placed into their appropriate place in the time series "by eye." It is important to note that affected were the data of 2 subjects only and fewer than 10 points per cycle (usually much fewer).

system (θ_i) was calculated for each sample (90/s) of the position time series to produce a time series of θ_i. The phase angles of wrist pendulum i at sample j (θ_{ij}) were calculated as

$$\theta_{ij} = \arctan\left(\frac{\dot{x}^*_{ij}}{\Delta x_{ij}}\right), \quad (11)$$

where $\dot{x}^*_{ij}$ is the velocity of the time series of wrist pendulum i at sample j divided by the mean angular frequency for the trial, and Δx_{ij} is the position of the time series at sample j minus the average position for the trial. The relative phase angle (Φ_i) between the two coupled wrist-pendulum systems was calculated for each sample as the $\theta_{\text{right}\,j} - \theta_{\text{left}\,j}$. The Φ_i that the subject intended to produce should be 0° for $\Phi_\Psi = 0°$ and 180° for $\Phi_\Psi = 180°$. The Φ time series allows an evaluation of how the subject satisfied this task demand. The evaluation was accomplished in a number of ways. First, the mean Φ was calculated for each trial and condition. Second, in order to determine the magnitude and patterning of the variability associated with this time series, a power spectral analysis was performed on the Φ time series. A 60-s time series was broken up into nine subsidiary time series each of 1,024 samples and each overlapping by 512 samples. Each subsidiary time series was windowed using a Welch filter to reduce spectral leakage, and all of the nine spectra from a given trial were averaged to reduce the error of the spectral estimate (Press, Flannery, Teukolsky, & Vetterling, 1988). Finally, the total power of Φ was calculated for each trial by summing the power at each frequency of the averaged spectra except the DC component at the zero frequency. This measure was used as a summary of the variability of Φ.

Results and Discussion

Frequency of Oscillation

The mean frequency of oscillation for each condition was submitted to a 2 × 3 × 5 analysis of variance (ANOVA) within factors of coordination mode (Φ_Ψ = 0 or 180), frequency condition (comfort frequency, 0.93 Hz or 1.15 Hz) and coupled pendulum system (1–5) in order to verify that the prescribed frequency of oscillation was actually performed. The only significant effect that the analysis yielded was a main effect for frequency, $F(2, 8) = 20.94$, $MS_e = 0.08$, $p < .01$. Figure 4 (upper panel) displays the mean frequencies performed, averaged across the coordination modes for each coupled pendulum system at each frequency condition. The observed frequencies of the 1.15-Hz and 0.93-Hz conditions were constant across system conditions with means that were near the metronome specified values (1.151 and 0.936, respectively), whereas the frequencies of the comfort mode were more variable but not significantly different from one another: Frequency Condition × Pendulum System, $F(8, 32) = 1.10$, $MS_e = 0.005$, $p > .05$.

Still, the variability of the coupled pendulum system frequencies in the comfort mode condition can be rationalized by Kugler and Turvey's (1987) virtual system hypothesis, namely, that the comfort frequency of a coupled wrist-pendulum system is dependent upon the magnitude of the two wrist-pendulum systems inertial loadings, in particular, the distance to their center of oscillation or virtual length (L_v). The formula for virtual length is

$$L_v = (M_1L_1^2 + M_2L_2^2)/(M_1L_1 + M_2L_2), \quad (12)$$

where M_1, L_1 refer to the mass and length, respectively, of one of the wrist-pendulum systems considered as a simple pendulum and M_2, L_2 refer to the mass and length of the other wrist-pendulum system considered as a simple pendulum. Given the symmetry of the wrist-pendulum pairings used (see Table 2), the five coupled systems had only three L_v values: 0.524 m (Systems 1 and 5), 0.535 m (Systems 2 and 4) and 0.618 m (System 3). As seen in Figure 4 (lower panel), the fact that the mean oscillation periods (1/frequency) calculated across the five subjects scale as a log linear function of the L_v is consistent with the Kugler and Turvey theory (see also Turvey, Schmidt, Rosenblum, & Kugler, 1988).

Deviation of Mean Φ From Φ_Ψ

The deviation of mean Φ from Φ_Ψ was calculated by subtracting the intended relative phase angle for each Φ_Ψ condition (0° or 180°) from the mean Φ of each trial. This transformation was performed in order to compare the attained Φ for the two coordination modes with each other relative to the goals of their respective conditions. On these magnitudes, a three-way ANOVA of the same design as above was performed. The analysis revealed no significant effects with coordination mode but a significant main effect for coupled pendulum system, $F(4, 16) = 64.57$, $MS_e = 524.27$, $p < .001$, and a significant interaction between frequency condition and coupled pendulum system, $F(8, 32) = 2.46$, $MS_e = 194.95$, $p < .05$. Figure 5 displays the mean deviation from Φ_Ψ averaged across the coordination modes for each system at each frequency condition. Two characteristics can be observed. First, as the $\Delta\omega$ values of the coupled pendulum systems deviate from zero, the deviation from Φ_Ψ increases. The conventions for the calculations of $\Delta\omega$ and Φ are that the left-hand values are subtracted from the right hand. Consequently, these deviations from Φ_Ψ can be interpreted as follows: The wrist-pendulum with the higher gravitational frequency (right when $\Delta\omega > 0$, left when $\Delta\omega < 0$) leads the other wrist-pendulum system in the cycle. (When right leads, deviation from $\Phi_\Psi > 0$; when left leads, deviation from $\Phi_\Psi < 0$.) Second, the magnitude of this lagging and leading is scaled by the magnitude of $\Delta\omega$ in a nearly linear fashion.

Figure 5 also shows that the scaling of the deviation from Φ_Ψ by the control parameter $\Delta\omega$ is different for the different frequency conditions. This significant interaction between frequency condition and coupled pendulum system is a consequence of the differences of the frequency conditions at $\Delta\omega = .386$ and $\Delta\omega = -.386$. Post-hoc t tests revealed significant differences between comfort mode frequency and the metronome scaled conditions for $\Delta\omega = .386$ (both $p < .01$) and between the comfort mode frequency and 1.15 Hz condition for $\Delta\omega = -.386$ ($p < .05$). In both cases, the comfort mode deviation from Φ_Ψ was smaller than that of the metronome paced conditions.

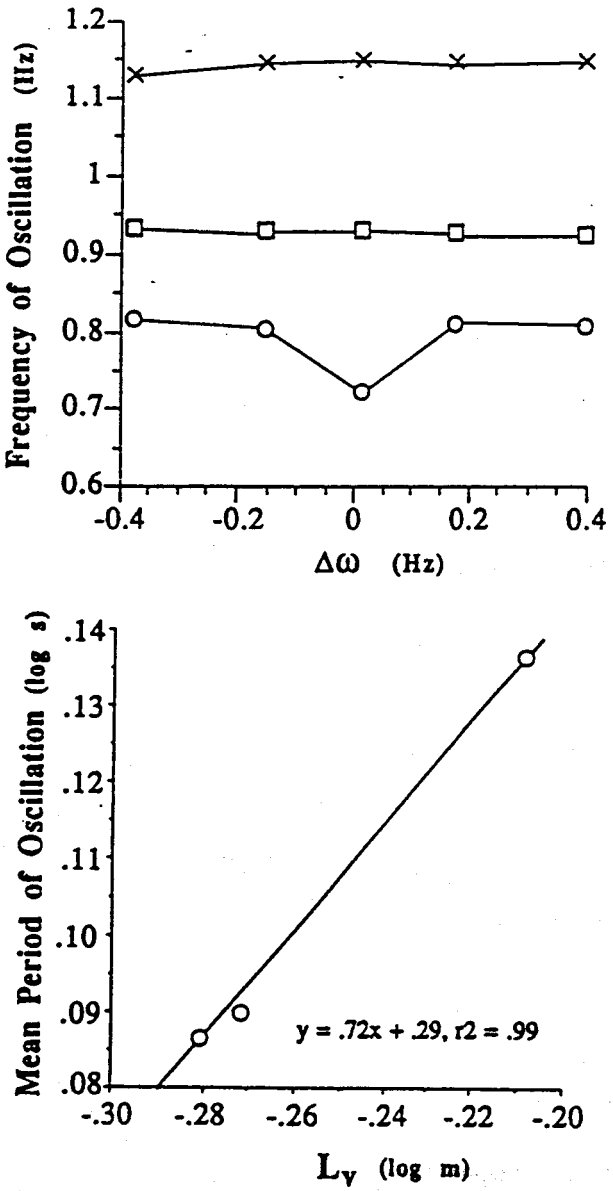

Figure 4. The upper panel demonstrates the frequency of oscillation ω_c that was attained across changes of the control parameter $\Delta\omega$ for the three ω_c conditions (circles = comfort frequency, squares = 0.93 Hz, crosses = 1.15 Hz). The lower panel displays the scaling between the ω_c in comfort mode and L_γ (the distance to the center of oscillation of the two coupled wrist-pendulum systems treated as a rigidly coupled system), as predicted by Kugler and Turvey (1987).

As argued in the introduction, according to a dynamical systems model of coupled oscillators, the deviation from Φ_Ψ with the scaling of the left-right imbalance ($\Delta\omega$) can be explained in terms of the displacement of the point attractor of Φ. One of the motivations of the present experiment was to see how this change of location in the Φ equilibrium point is affected by the scaling of another control parameter, ω_c. The scaling of the ω_c seems to exaggerate the deviation from Φ_Ψ in pendulum systems with relatively large $\Delta\omega$. To the extent that the displacement of the attractor point away from Φ_Ψ can be seen as an approach to unstable relative phase values (e.g., 90°), the scaling of ω_c can be interpreted as adding to the destabilization produced by the scaling of $\Delta\omega$.

The candidate dynamical system models of coupled oscillators presented in the introduction (Equations 7 and 8) can be fit to the present data; assuming $\dot{\Phi} = 0$, using a regression technique. With $\Delta\omega$ as a dependent variable and $\sin(\Phi)$ and $\sin(2\Phi)$ as independent variables, a stepwise regression can be used to establish the model (i.e., combination of these independent variables) that best fits the data. Analyses were performed separately on the data from the three frequency conditions. Since there was no effect of coordination mode, the data from the two conditions were combined. For the two metronome-scaled conditions (0.93 Hz and 1.15 Hz), the $\sin(\Phi)$ term was significant–0.93 Hz, $t(47) = 2.65$; 1.15 Hz, $t(47) = 4.76$, both $p < .05$–whereas the $\sin(2\Phi)$ term was not—0.93 Hz, $t(47) = 1.35$; 1.15 Hz, $t(47) = 1.40$, both $p > .05$. In the comfort mode frequency condition, the $\sin(2\Phi)$ term was significant, $t(47) = 2.34$, $p < .05$, whereas the $\sin(\Phi)$ term was not, $t(47) = 0.07$, $p > .05$.

The $\sin(\Phi)$ model of Rand et al. (1988) (Equation 8) is the best fit model for the two metronome scaled frequency conditions ($r^2 = .85$ and $r^2 = .88$, respectively) whereas a single-term $\sin(2\Phi)$ is the best fit for the comfort mode condition ($r^2 = .77$). However, because the $\sin(2\Phi)$ term is not in itself a model and the simple regression of $\sin(\Phi)$ on $\Delta\omega$ presents a competitive correlation ($r^2 = .75$), the model of best fit for all three conditions will be taken to be the $\sin(\Phi)$ model found in Equation 8. The fit of this model to the data of the three frequency conditions can be seen in Figure 6. The slope of the regression of

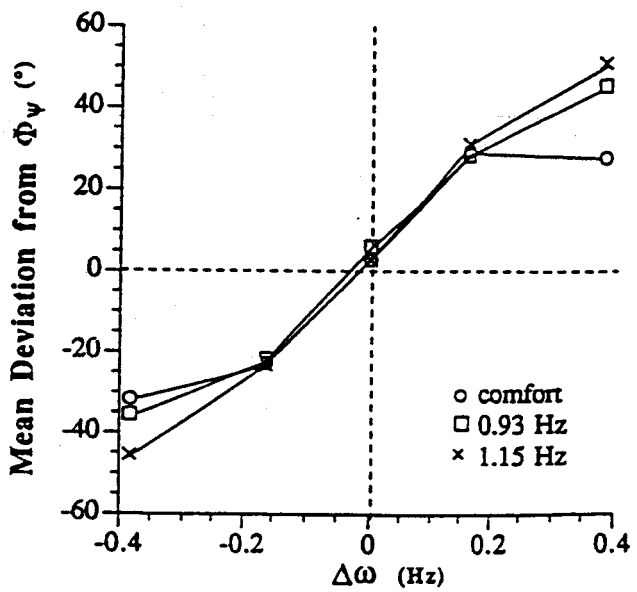

Figure 5. The mean deviation from intended relative phase (Φ_Ψ) attained across changes of the control parameter $\Delta\omega$ for the three ω_c conditions.

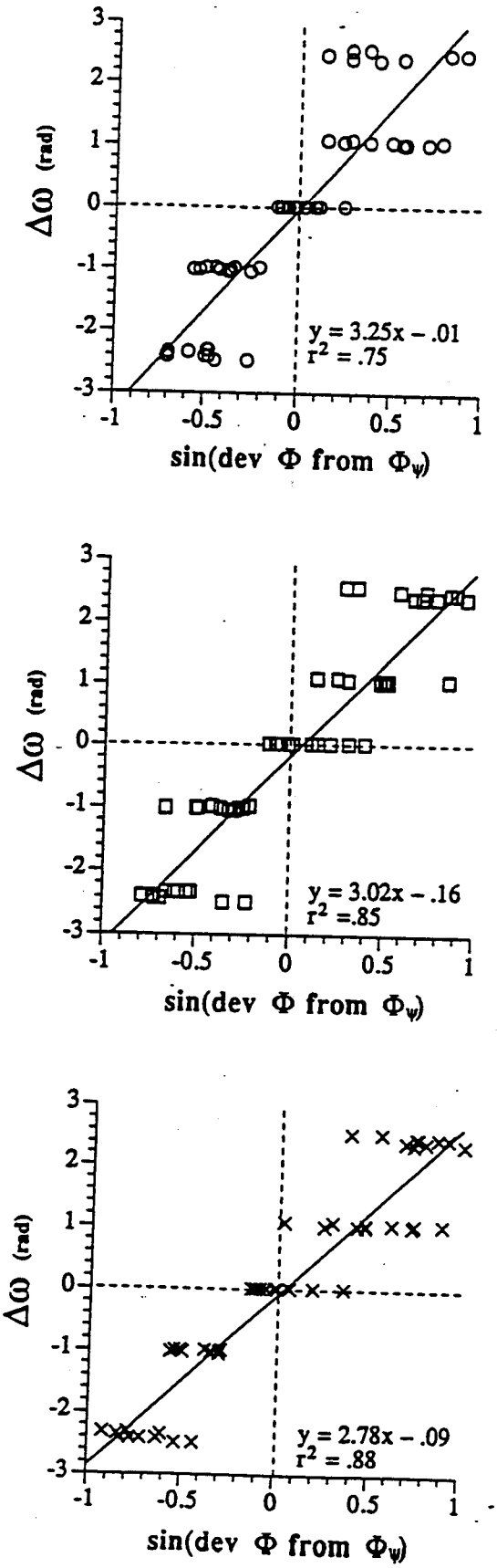

Figure 6. The fit of the Rand et al. (1988) model found in Equation 8 to the observed deviations from Φ_Ψ. (The upper, middle, and lower panels shows the fit of this model to the data of the comfort mode, 0.93-Hz and 1.15-Hz conditions, respectively.)

sin(Φ) on $\Delta\omega$ can be interpreted as the coupling term k in this equation. In regressions performed separately on the data of the three frequency conditions, the following ks were found: 3.25 for the comfort condition, 3.02 for the 0.93-Hz condition and 2.78 for the 1.15-Hz condition.

These results indicate that increasing the control parameter ω_c can be interpreted as having the effect of decreasing the magnitude of the coupling strength of the coupled oscillator models of Φ in Equations 7 and 8. This scaling was assumed in the modeling of Haken et al. (1985) but until now has not been empirically measured. As stated in the introduction, decreasing the coupling strength in this model would have the effect of increasing the instability of the system by making the attractor region more shallow and lead ultimately to its breakdown when k passes through a critical value that depends upon $\Delta\omega$. Because increasing ω_c decreases the coupling strength and the stability of the attractor, we may anticipate observing greater fluctuations in Φ as ω_c is increased. Tests of this prediction are presented in the next section.

Patterning of the Relative Phase Spectrum

The spectral analysis of Φ allows us to determine the magnitude and patterning of fluctuations found in the Φ time series across the different frequency ranges. Figure 7 demonstrates the spectral analyses of the 30 trials of a representative subject. The spectra are plotted in normalized coordinates where, on the abscissa, the frequency is scaled to the ω_c and, on the ordinate, the power is scaled to the total power. Two qualitative features previously noted by Schmidt et al. (1991) are apparent. First, the spectra have a local patterning of power in spectral peaks at integer multiples of the oscillation frequency. Second, they have a general hyperbolic shape such that the power scales to $1/f$, where f is the spectral frequency. Following Schmidt et al. (1991), a number of analyses of the spectral patterning are pursued in the following sections to see how the local (peaks) and global ($1/f$) qualitative features of the spectra change with the two control parameters, ω_c and $\Delta\omega$, and $\Phi_\Psi = 0°$ or 180°.

Total power of Φ. The total power of Φ is a summary measure of fluctuation in relative phase exhibited across the entire range of possible frequencies. A three-way ANOVA with the same design as those before was performed on the log transform of total power. This analysis revealed a significant main effect of coordination mode, $F(1, 4) = 249.59$, $MS_e = 0.004$, $p < .001$, which demonstrates that there were more fluctuations when $\Phi_\Psi = 180°$ (3.24) than when the $\Phi_\Psi = 0°$ (3.08). However, analysis of a significant Coordination Mode × Coupled Pendulum System interaction, $F(4, 16) = 3.27$, $MS_e = 0.03$, $p < .05$, indicates that this difference between the relative phase modes exists only at the $\Delta\omega$ values near 0 ($\Delta\omega = 0$ and

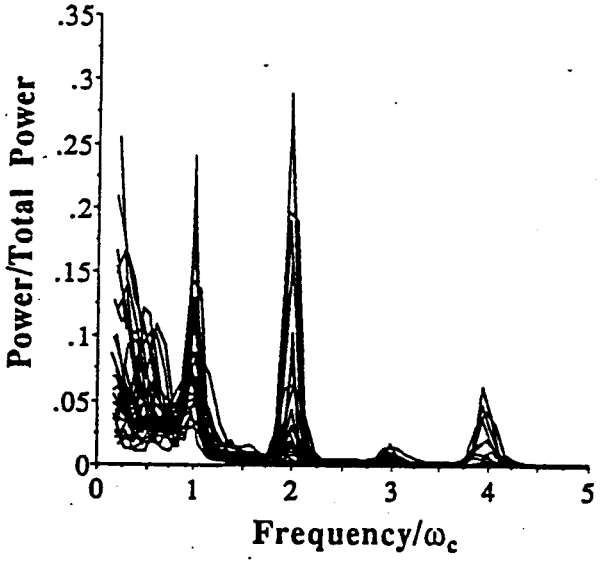

Figure 7. The normalized spectra of Φ for the 30 trials of a representative subject.

±.164) and not for the systems with extreme left–right imbalances ($\Delta\omega = \pm .386$).

Main effects for both frequency condition and coupled pendulum system were also significant, $F(2, 8) = 6.83$, $MS_e = 0.14$, $p < .05$, and $F(4, 16) = 16.04$, $MS_e = .06$, $p < .001$, respectively, which indicates that in general the fluctuations increased as $\Delta\omega$ deviated from zero and when ω_c deviated from the comfort mode. However, as Figure 8 (upper panel) portrays, there is a complicating significant interaction between frequency condition and coupled pendulum system, $F(8, 32) = 5.62$, $MS_e = .04$, $p < .001$. A simple effects analysis reveals that the basis for this interaction is significant system effects for the comfort and 0.93-Hz frequency conditions (both $p < .001$) but not the 1.15-Hz condition ($p > .05$). For the comfort and 0.93-Hz frequency conditions, the variability in interlimb coordination increased as $\Delta\omega$ deviated from 0; but in the highest ω_c condition, no matter what the left–right imbalance ($\Delta\omega$), the interlimb phasing had the same amount of variability.

A consequence of this effect is that the total power becomes more equal for the three ω_c conditions as $\Delta\omega$ deviates from 0. This is born out in post hoc t tests comparing the marginal means plotted in Figure 8 (upper panel). At $\Delta\omega = 0$, the three frequency conditions are significantly different from each other ($p < .05$); but at the other $\Delta\omega$s, only one pair of means are significantly different (at $\Delta\omega = -.164$, the comfort and the 1.15-Hz conditions; at $\Delta\omega = .164$, the 0.93-Hz and the 1.15-Hz conditions; and at $\Delta\omega = \pm .386$, the comfort and the 0.93-Hz conditions, all $p < .05$).

In sum, fluctuations in Φ as indexed by the total power in general are greater for the alternate mode of relative phasing and for higher-frequencies of oscillation. However, these effects depend upon the left–right imbalance of the pendulum involved: As the coupled pendulum systems' $\Delta\omega$ deviates from 0, the interlimb phasing variability of the two coordination modes becomes less different

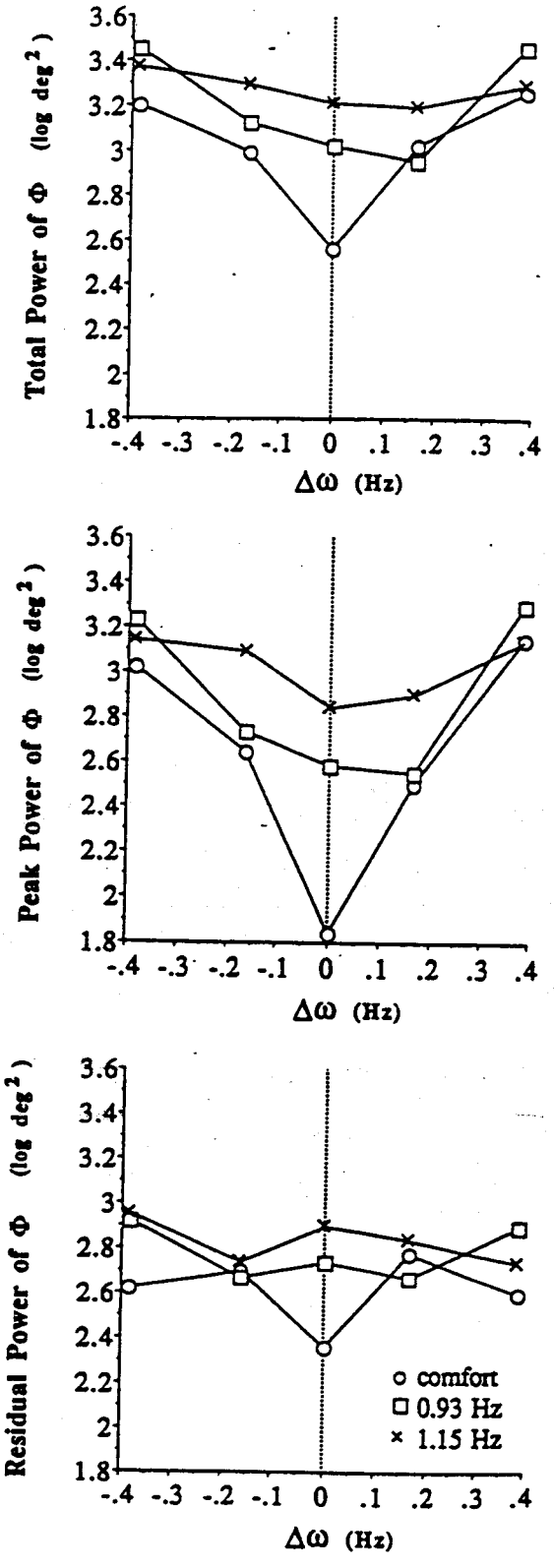

Figure 8. The spectral power of Φ as a function of the control parameter $\Delta\omega$ for the three ω_c conditions. (The upper, middle, and lower panels display the total power, the peak power, and the residual power, respectively.)

(the Φ fluctuations of the symmetric mode becomes more like the alternate mode) as does the variability of the different frequency conditions (the Φ fluctuations of the comfort mode becomes more like the 0.93-Hz and 1.15-Hz conditions).

Can the dynamical system of Equation 8 model the observed variability of Φ? Given that the fluctuations observed in a dynamical system will increase with the time it takes for the system to relax to equilibrium from a perturbation—its relaxation time—the fit of the data to this model can be assessed by calculating the relaxation time for the model given the specific parameters found in the experimental situation. The relaxation time of the regime can be determined for the candidate magnitudes of k (3.25 for comfort, 3.02 for 0.93 Hz, and 2.78 for 1.15 Hz) and the candidate values $\Delta\omega$ (.386, .164, 0, −.164, −.386) through numerical integration of this equation given an initial perturbation from the regime's stable attractor point (20°).

On average, in concert with the data, these relaxation times increase as the ω_c increased from comfort mode (1.27 s, 1.58 s, 2.56 s for comfort, 0.93-Hz and 1.15-Hz conditions) and as the pendulums system deviated from $\Delta\omega = 0$ (2.94 s, 1.07 s, 1.00 s for $\Delta\omega = \pm.386, \pm.164$, and 0). The relation between the relaxation times and the magnitudes of the observed total power of Φ can be seen in Figure 9 (top). The relaxation times determined through Equation 8 are fair predictor of the total power found empirically. There is a linear relation between the two variables, $r^2(14) = .32$, $p < .05$. The graph indicates that the relaxation time for the extreme $\Delta\omega$ six coupled pendulum systems (1.73 s, 2.34 s, 4.69 s for the three ω_c conditions) should have been much smaller given the magnitude of fluctuations observed. Indeed, relaxation times that large probably too long to produce stable coordinated interlimb phasing. Scholz et al. (1987) found that as the relaxation time of bimanual phasing of limbs approaches 1.3 s, a breakdown occurs in the coordination. The model predicted values for extreme $\Delta\omega$ are in excess of this empirically derived limit.

Assuming that this limit for the relaxation time cannot be exceeded, Figure 9 (bottom) replots the total power as a function of the model predicted relaxation time where for the extreme values of $\Delta\omega$ the relaxation time is set to 1.2 s. The increased correlation of the relaxation time and total power, $r^2(14) = .78$, $p < .001$, suggests that the relaxation times of the observed control structure probably do not exceed 1.2 s. How can the limit on the relaxation time be understood in terms of the dynamical model in Equation 8? It may be that as the increased left–right imbalance makes the coordination harder and harder to maintain, additional control processes are used besides those expressed in Equation 8 that effectively decrease the relaxation time of the control structure for extreme $\Delta\omega$ values and, thereby, increase the stability of the coordination. In short, additional control processes may be used to decrease the relaxation time of the dynamic instantiated by Equation 8. That this is the case is further substantiated by how the power is

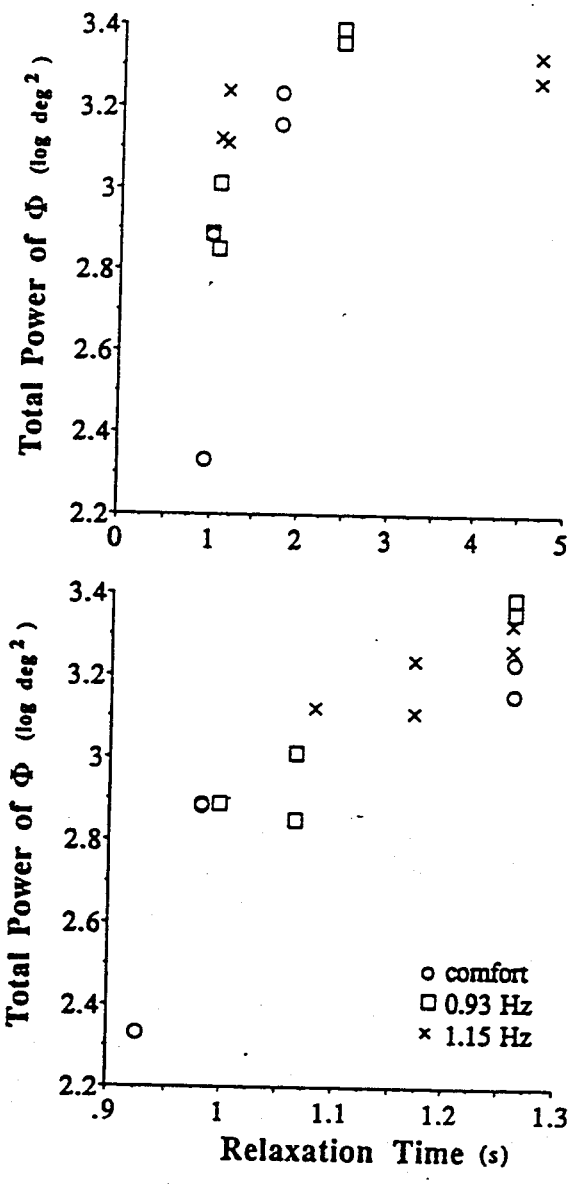

Figure 9. The relationship between the relaxation time predicted by Equation 8 and the total power of Φ observed for the data of the comfort mode, 0.93-Hz and 1.15-Hz ω_c conditions. (The upper panel displays the relaxation times predicted directly from the model given the parameters derived from the present experiment. The lower panel displays the relaxation times that respect the empirically derived limit for stable phasing, 1.2 s, found by Scholz, Kelso, and Schöner, 1986.)

spread across the frequencies of the spectrum. This is explored in the analyses of the next section.

Peak power and residual power in the Φ spectrum. The total power of the Φ spectra can be divided into two components: The power found in the spectral peaks at integer multiples of the frequency of oscillation (ω_c) and the residual power that is not at these peaks. In order to determine the effects of ω_c, $\Delta\omega$, and Φ_Ψ on these two different kinds of fluctuations, an algorithm was used to find the magnitude of the power to be found solely at the spectral

peaks. To account for the fact that these peaks had a band width, the power at the peak, the power at one frequency bin above and below, were summed to estimate the peak power of a spectrum. The difference between the total power of a spectrum and its peak power is the residual power of the spectrum. The frequency distributions of the spectral frequency at which the peaks were found are plotted in Figure 10 for the two coordination modes. The distributions do not appear dramatically different for Φ_Ψ = 0° and Φ_Ψ = 180°. In both cases, the spectral peaks tend to appear at integer multiples of ω_c and the number of peaks decreases as the spectral frequency increases. As can be observed in Figure 10, although the majority of the peaks are at integer multiples of the ω_c, a portion of them are not. These nonharmonic peaks may be due to the variability in the estimate of ω_c. There is no doubt that some variation in the ω_c occurred across the 60 s of a trial (especially for the comfort mode); hence, the mean ω_c for the entire trial may not be the ω_c for the portion that generated the apparently nonharmonic spectral peak.

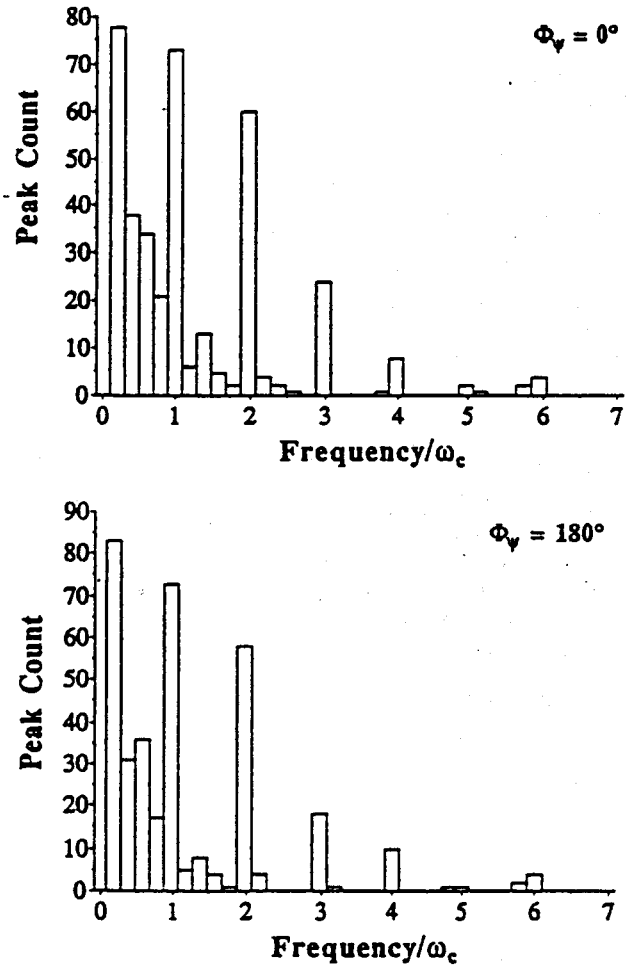

Figure 10. The distribution of the spectral frequencies at which peaks occurred for the Φ_Ψ = 0° coordination mode (top panel) and Φ_Ψ = 180° coordination mode (lower panel).

A three-way ANOVA with the same design as those previous was performed on the log transform of the peak power. The array of significant effects was very similar to those in the analysis of total power. The ANOVA yielded significant main effects of frequency condition, $F(2, 8) = 9.36$, $MS_e = 0.21$, $p < .01$, and coupled pendulum system, $F(4, 16) = 23.69$, $MS_e = 0.13$, $p < .001$. The peak power increased as the $\Delta\omega$ deviated from 0 and as ω_c increased from comfort mode. The coordination mode main effect was not significant ($p > .05$). The middle panel of Figure 8 (which looks nearly identical to the upper panel) displays a significant interaction between frequency condition and coupled pendulum system, $F(8, 32) = 4.81$, $MS_e = 0.10$, $p < .001$. A simple effects analysis reveals much the same asymmetry in the effect of coupled pendulum system condition as with the analysis of total power: For the comfort and 0.93-Hz conditions, the variability in interlimb coordination increased as $\Delta\omega$ deviated from 0; but in the 1.15-Hz condition, regardless of the values of $\Delta\omega$, the interlimb phasing had a great amount of variability. Again, as with the total power, post hoc *t* tests reveal that the peak power become more equal for the three ω_c conditions as $\Delta\omega$ deviates from 0.

An identical ANOVA was performed on the log transform of the residual power. The analysis produced a significant effect of coordination mode only, $F(1, 4) = 12.02$, $MS_e = 0.08$, $p < .05$. The means of residual power calculated across coordination modes are displayed in the lower panel of Figure 8 so that the data can be compared with the total (upper panel) and peak power (middle panel). It is obvious from inspection of these graphs that the magnitude of the residual power is relatively depressed and undifferentiated by the frequency and coupled pendulum system conditions.

The conclusion can be drawn that the effects of the control parameters $\Delta\omega$ and ω_c are mainly on the magnitude of the power at the peaks in the spectra rather than the residual power. However, the effect of the coordination mode Φ_Ψ appears to effect mainly the magnitude of the residual power. The implication is that the kind of fluctuations that are scaled by the control parameters are harmonically organized fluctuations or rhythmicities in the behavior of Φ, whereas, the kind of fluctuations that are effected by the coordination mode are more stochastic in nature. The coordination mode fluctuations are in line with what the dynamical system in Equation 8 would predict for fluctuations in Φ. The control parameters fluctuations, however, go beyond what Equation 8 would predict. This model does not predict any packaging of Φ fluctuations into periodicities but only that the fluctuations should increase with deviation of $\Delta\omega$ from 0 and with decreases in the coupling strength *k*. In order to produce the periodic behavior of Φ, other control processes must be added to this regime.

The topology of the spectral peaks. In Schmidt et al. (1991), a multiple regression analysis found that the power at the peaks was structured in a particular fashion. They found an inverse log-linear relationship between peak height and spectral frequency with peaks at lower spectral frequencies being larger than those at higher spectral fre-

quencies. This topology reflects the general nature of the spectra of Φ to exhibit a $1/f^{\delta}$ shape (see below). The regression analysis also found that the height of the peaks changed in a direct log-linear relationship with the distance from $\Delta\omega = 0$: The larger the deviation from $\Delta\omega = 0$, the larger were the spectral peaks. The consequence of these two relations is that new peaks come into existence at higher frequencies as $\Delta\omega$ deviates from zero more and more. This previous study suggested that the emergence of new spectral peaks is evidence for the genesis of new functional subtasks (e.g., more perceptual pickup processes) in the dynamical regime underlying the interlimb coordination that are required as the scaling of the control parameter $\Delta\omega$ makes the coordination more difficult.

The question that remains is whether the same relations (that the height of the peaks scale to $1/f$ and to $\Delta\omega$) hold for the present data and whether these relations are affected by the coordination mode Φ_Ψ and the control parameter ω_c. To this end, a multiple regression analysis was performed with a dependent variable of log peak power, with continuous independent variables of $|\log \Omega|$ (where $\Omega = \omega_{left}/\omega_{right}$ is used instead of $\Delta\omega$ for comparison to Schmidt et al., 1991) and log peak number (integer multiple of oscillation frequency, 1–5) and with categorical independent variables of frequency condition and coordination mode. The analysis did not reveal a main effect of coordination mode ($p > .05$). This indicates that the topology of the Φ spectra did not differ for $\Phi_\Psi = 0°$ and $\Phi_\Psi = 180°$ and was anticipated by the similarity of the distribution of spectral peaks displayed Figure 10.

In short, this result shows that the topological packaging of the fluctuations of Φ does not differ for the two coordination modes. This is interesting because it has been proposed that the difference in the stability of the attractors at $\Phi = 0°$ and $\Phi = 180°$ are a consequence of the differences in the information availability for the two coordination modes (Kugler, 1990). That is, information about whether the two limbs are coordinated is available only at peak flexion and extension in alternate mode but is continually available for the symmetric mode. Hence, because the number of possible control or "synch" points within a cycle is greater for symmetric than the alternate phase mode, the symmetric mode is inevitably more stable. Furthermore, Schmidt et al. (1991) suggest that the peaks of the Φ spectrum may index the number of control points used within a cycle to maintain the coordination. If (a) the difference in the stability of the two coordination modes is a consequence of the difference in the availability of information and (b) the peaks in the spectrum represent perceptual pickup processes, then one would have expected the topology of peaks of the Φ spectra to differ for the $\Phi_\Psi = 0°$ and $\Phi_\Psi = 180$. Because this did not occur, one of these two assumptions (or both) may be incorrect.

Significant main effects were found for the two continuous variables, $|\log \Omega|$, $F(1, 867) = 5.83$, $MS_e = 0.003$, $p < .001$, and log peak number, $F(1, 867) = 2{,}618.02$, $MS_e = 0.003$, $p < .001$. The coefficients (slopes) of the latter two effects were 5.07 and −3.02, respectively, demonstrating once again (a) the direct log-linear relation between the control parameter Ω (viz., $\Delta\omega$) and the height of the peaks and (b) an inverse log-linear relation between the frequency and peak height. The latter result demonstrates that the $1/f$ nature of the spectrum (see next section) is apparent in the spectral peaks. The former result indicates that as the control parameter $\Delta\omega$ deviates from 0 that new peaks at higher frequency multiples come into existence (see Schmidt et al., 1991, Figure 9).

A significant main effect was also found in this the multiple regression analysis for the categorical variable of ω_c, $F(1, 867) = 309.14$, $MS_e = 0.003$, $p < .001$. Multiple regressions of $|\log \Omega|$ and log peak number on log peak power for the data of the three frequency conditions separately produce the regression equations displayed in Table 3. Inspection of this table reveals that the intercepts of the regressions increase as the ω_c changes from comfort mode to 0.93 Hz to 1.15 Hz, which indicates that the topology of the power across the different peaks and $|\log \Omega|$ does not change but is simply raised as the control parameter ω_c is increased. In short, the peaks become larger as ω_c is increased. This raising of the spectrum has the effect of producing new peaks at higher frequency multiples as the ω_c is increased.

To reiterate, the spectral peaks of the Φ spectrum can been interpreted as representing control processes that package the ensuing instability of the dynamical regime assembled to govern the coordination. It has been suggested that these processes may be control points at different parts of the cycle where informational pickup occurs to ensure control of the coordination (Beek, 1989). The current results indicate that as the left–right imbalance of the coupled pendulum systems (i.e., $\Delta\omega$) increases and as the frequency of oscillation increases (ω_c), the spectral peaks increase in their number. These results, given the above working hypothesis, suggest that new perceptual tuning processes are brought to bear as the control parameters make the coordination more difficult. How this working hypothesis can be directly tested is suggested in the General Discussion section.

$1/f^{\delta}$ patterning of power. In order to investigate the global topology of the Φ power spectrum, simple regressions of log power of the entire spectrum on log (spectral) frequency were performed to estimate the $1/f^{\delta}$ nature of the spectrum. The absolute values of the regression coefficients are estimates of the δ exponent of the $1/f$ topology. The values were submitted to three-way ANOVA with the same design as those used previously to determine how the two control parameters, ω_c and $\Delta\omega$, and the coordination

Table 3
Summary of the Multiple Regression of $|\log \Omega|$ and Log Peak Number on Log Peak Power at Each Frequency Condition

Frequency condition	$\lvert\log \Omega\rvert$ coefficient	Log peak number coefficient	Intercept	r^2
Comfort	7.22	−3.17	0.62	.83
0.93 Hz	5.87	−2.88	1.12	.71
1.15 Hz	2.12	−3.01	1.52	.76

mode affect the global form of the spectra. The analysis indicated a significant main effect of coupled pendulum system, $F(4, 16) = 7.47$, $MS_e = 0.18$, $p < .01$, but no other significant effects.

In order to evaluate this coupled pendulum system effect, Ω ($= \omega_{left}/\omega_{right}$) was regressed on the δ exponent of the $1/f$ topology. Again Ω was used to allow comparison with the analyses in Schmidt et al. (1991). A plot of this analysis is displayed in Figure 11 demonstrates a quadratic relation between Ω and δ ($\delta = 1.74 + 2.16\ \Omega - .80\Omega^2$), $r^2(141) = .07$, $p < .01$. The δ exponent decreases in magnitude on either side of a maxima at $\Omega = 1.35$. This result replicates that of Schmidt et al. (1991); as a matter of fact, the regression weights are very similar those observed in that study. The correlation of the present study is much less than that of the former, however. One reason for this may be that the previous study used coupled pendulum systems with a much wider range of left–right imbalance (Ω = .38 to 1.98 vs. .62 to 1.63 in the present study) and with many more different values of Ω (~100 vs. 5).

Interpreting the structure of the spectra from the spectroscopic perspective of homeokinetics (Iberall, 1977, 1978) that maintains that biological organisms are unified concatenations of rhythmic subsystems stratified across many space/time scales, the $1/f$ distribution of power of the Φ spectrum indexes the relation between the subtasks that underlie the rhythmic coordination. The $1/f^{\delta}$ distribution of power seem to be a universal biological design feature that indicates a scale invariant distribution of energy across subsystems at different space–time scales. As stated above, the δ of the $1/f^{\delta}$ scaling is indicative of the amount of correlation between the subtasks of a system. As δ increases, there is an increasing amount of correlation between the subtasks because more power will be concentrated in one particular part of the spectrum (the lower frequencies). The decrease of δ magnitudes with increases in left–right imbalance (deviation of $\Delta\omega$ from 0 or Ω from 1) indicates that the correlations between the subtasks decrease as the eigenfrequencies of the component oscillators become more different.

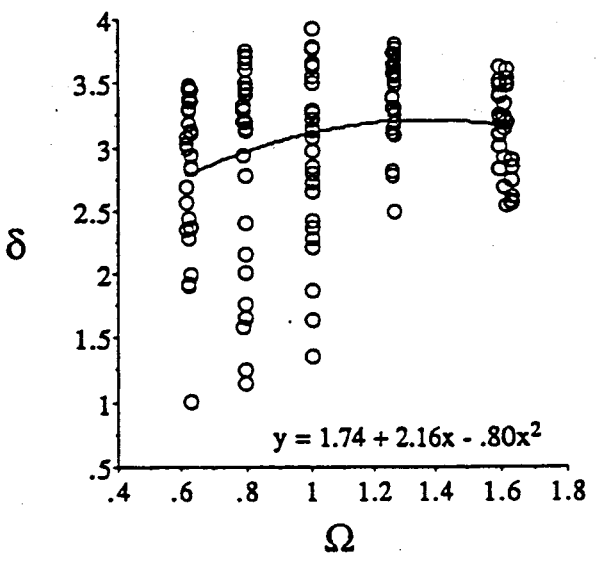

Figure 11. The magnitude $1/f$ exponent δ of the Φ spectra as a function of the control parameter Ω ($= \omega_1/\omega_2$).

General Discussion

The present results verify that interlimb phasing of two rhythmic movements can be understood as being governed by general dynamical principles. The patterning of the indices of interlimb coordination, mean relative phase and power of relative phase (Φ), changed with the independent variables, frequency of oscillation (ω_c), left–right system imbalance ($\Delta\omega$) and intended coordination modes (Φ_Ψ), in ways that can be interpreted from the dynamical model presented in Equation 8.

Whereas past studies have demonstrated the independent effects of ω_c and $\Delta\omega$ on interlimb phasing and the dynamical nature of the control structure underlying this phasing, the present work has investigated the effects of simultaneous manipulation of these variables. It has been shown that the effects of these control parameters on the mean Φ and the general variability associated with Φ (i.e., total power of Φ) can be understood in terms of a single model. However, other observed properties of the patterning of Φ, namely the global and local structure of the Φ spectrum, cannot be understood in terms of any extent dynamical model of interlimb coordination. The spectral peaks at integer multiples of the frequency of oscillation represent how the control structure governing interlimb phasing reacts to growing instability. The distribution of the power in the spectrum is not random but becomes concentrated at specific spectral frequencies. That is, there are rhythms in the behavior of the relative phase angle. These periodicities indicate that the coordination is not one of phase locking but phase entrainment. This phase entrainment patterning can be explained by modifying the present dynamical model of Equation 8. In the following remarks, a summary of the results is elaborated and modifications of the dynamical model are suggested.

Summary of Results

The effects of the left–right imbalance control parameter $\Delta\omega$ found in previous studies were for the most part replicated here. As $\Delta\omega$ deviated from 0, an increase was found in the deviation of Φ from Φ_Ψ (Figure 5) and the total power and peak power (Figure 8 top and middle) but not residual power (Figure 8 bottom) of the Φ spectrum (Rosenblum & Turvey, 1988; Schmidt et al., 1991; Turvey et al., 1986). Furthermore, as $\Delta\omega$ deviated from 0, spectral peaks grew in height at lower spectral frequencies and new spectral peaks emerged at higher ones (Schmidt et al., 1991). Also, the exponent δ of the $1/f^{\delta}$ nature of the spectrum was found to decrease in magnitude (Figure 11) as $\Delta\omega$ deviated from 0 (Schmidt et al., 1991). The dynamical model of Equation 8 predicts both the mean deviation of Φ from Φ_Ψ (Figure 6) and the increase in the total power of the Φ spectrum (Figure 9).

The effects of the coordination mode are also in line with past studies which have found the alternate phase mode to be less stable than the symmetric phase mode (Kelso, 1984; Schmidt et al., 1990; Turvey et al., 1986). However, the present results verify that this differential stability is revealed only in some measures (Turvey et al., 1986). The coordination mode has an effect upon the magnitude of the total and residual power observed of the Φ spectrum but not the mean deviation from intended phase (Φ_Ψ), height of the spectral peaks, nor the δ of the $1/f$ topology of the Φ spectrum. The dynamical-model of Equation 8 predicts that the deviation from Φ_Ψ should be different for the two coordination modes if the spectral power (variance) of Φ is different for them. This does not appear to be the case: The deviation from Φ_Ψ ANOVA found the coordination mode effects not significant, whereas the total power ANOVA found the coordination mode effects to be significant. However, the mean coupling strengths for $\Phi_\Psi = 0°$ and $\Phi_\Psi = 180°$ when estimated through a regression analysis are found to be 3.03 and 2.94, respectively. The ordering of these values are in accord with the model's predictions.

In addition to $\Delta\omega$ and Φ_Ψ, the present study also investigated the simultaneous manipulation of the frequency of oscillation, ω_c. The effect of ω_c was uniform across both coordination modes. This may seem counterintuitive because previous studies have found that scaled increases in ω_c lead to a breakdown in the alternate but not the symmetric mode of relative phasing (Kelso, 1984; Kelso et al., 1986; Schmidt et al., 1990). The present results suggest that this effect of ω_c is a consequence of the differential stability of the two Φ modes at any ω_c rather than a differential stability of the two modes only at higher ω_c.

The scaling of control parameter ω_c was found to interact with the scaling of the control parameter $\Delta\omega$: ω_c increased the deviation from Φ_Ψ at extreme values of $\Delta\omega$ (Figure 5) and increased the magnitude of the total and peak power observed in the Φ spectrum for coupled pendulum systems with small left–right imbalances (Figure 8 top and 8 middle). More exactly, ω_c effect on mean deviation from Φ_Ψ was greatest at $\Delta\omega = -.386$ and .386, whereas its effect on the variability of Φ was least at those $\Delta\omega$ values and greatest at $\Delta\omega$ values near 0. The former effect can be directly predicted from the dynamical model of Equation 8 assuming that the increases in ω_c decrease the coupling strength k (Figure 6). The effect of ω_c on the total power is also predictable from Equation 8 if one assumes that the relaxation time of the dynamical control structure is held at a fixed limit by other control processes in addition to those in the present model (Figure 9, bottom). Just how the model can be revised to include additional control processes is outlined in the next section.

Revision of the Dynamical Model

In addition to the lower relaxation times, the model in Equation 8 fails to predict two aspects of the Φ spectrum: The power is locally concentrated at integer multiples of the ω_c as well as globally distributed in a $1/f^\delta$ fashion. Equation 8 makes no predictions about the structure of the variance

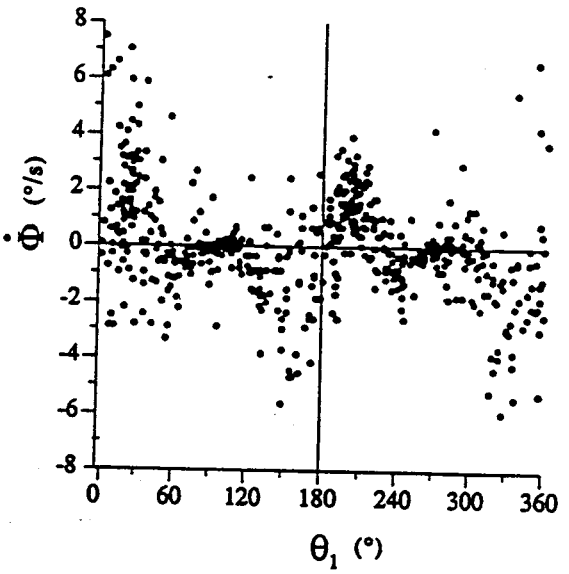

Figure 12. $\dot{\Phi}$ as a measure of the phase entrainment behavior that is indexed by the peaks of the Φ spectrum as a function of the phase angle of the left hand (θ_l).

around a stable relative phase angle Φ. However, there are ways that the model in Equation 8 may be modified to account for the properties of the spectral peaks and $1/f^\delta$ shape. To obtain the latter property, one can assume that high-dimensional noise encroaches upon the behavior of Φ from the multitudes of microscopic components that are making up the more macroscopic limb movements. This assumption was used by Schöner et al. (1986) in order to model the critical fluctuations observed immediately before the transition from $\Phi = 180°$ to $\Phi = 0°$ using Equation 7. They added a Gaussian noise term Q of constant force to Equation 7. This constant noise interacts with the concavity of the potential well such that fluctuations in Φ increase as the well becomes more and more shallow. A $1/f^\delta$ shape to the Φ spectrum may be observed if a noise term of a different form, not the symmetric Gaussian but an asymmetric lognormal one, is assumed. The magnitude of fluctuations at each frequency may then scale to the inverse of that frequency.

The spectral peaks can be interpreted as indicating that the behavior observed in the coordination variable Φ is not phase locking but phase entrainment behavior (Figure 3, upper panel). What needs to be predicted to capture the phase entrainment behavior is the rate of change of Φ or $\dot{\Phi}$. Figure 12 shows how $\dot{\Phi}$ is patterned with respect to the phase angle (θ) of the left hand in a given trial of approximately 60 cycles. Notice that the patterning in the first half of the cycle (0° to 180° or extension) almost repeats itself exactly in the second half of the cycle (180° to 360° or flexion) and that there are further subsidiary undulations within each half cycle. It is this kind of periodic behavior that is captured in the peaks of the spectrum of Φ. As stated in the introduction, Equation 8 can be modified to account for this phase entrainment in two ways: by making the coupling dynamic (H in Equation 6) more complicated and

asymmetric and by making the oscillatory dynamics of the individual rhythmic units different (F_i in Equations 1 and 2).

The former kind of modification is exemplified by a model of phase entrainment proposed by Keith and Rand (1984):

$$\dot{\Phi} = \Delta\omega + k_1 \sin(\theta_1 - \theta_2) - k_2 \sin(\theta_1 - 2\theta_2). \quad (13)$$

This dynamical regime has been shown to have both 1:1 and 2:1 phase entrainment. Furthermore, under specific parameterizations a bifurcation occurs between the two coordination modes. Notice that Equation 13 is Equation 8 with a second coupling term, $k_2 \sin(\theta_1 - 2\theta_2)$, added that represents a sinusoidal forcing at two times the frequency of oscillation. It seems reasonable that the spectral peaks observed in the Φ spectra may be due to a number of these higher order coupling functions that correspond to subsystem control processes that are appropriated to harness the ensuing variability. Given this possibility, the following model was fit to the $\dot{\Phi}$ time series to see if these terms capture the structure of the spectral peaks observed:

$$\dot{\Phi} = \Delta\omega + \sum_{i=1}^{6} k_i \sin(\theta_1 - i\theta_2). \quad (14)$$

A stepwise regression fit of the coupling terms to the flexion and extension $\dot{\Phi}$ behavior observed in Figure 12 was performed using time series from the 30 trials of each subject that were downsampled by 10 (600 points total). Significant fits to the model were found for about two thirds of the trials but many of these had low correlations. The mean correlation for the combined flexion and extension behavior was .17 (SD = .13). We would predict low correlations for the condition where $\Delta\omega = 0$ but an increase in the correlation as $\Delta\omega$ deviates from 0 because the relative peak power with respect to residual power (and, hence, phase entrainment behavior with respect to noise) increases in these conditions. The regression analysis shows that the model fit r^2 significantly increases with the deviation of $\Delta\omega$ from 0 ($y = .46x + .07$, $r^2 = .28$, $p < .05$), as would be expected.

Spectral analyses of the time series predicted by the model are compared in Figure 13 with spectra of two representative trials, one with $\Delta\omega = .368$ and one with $\Delta\omega = 0$. When $\Delta\omega$ is large, the model and observed spectra are qualitatively very similar. They have the same number of spectral peaks at the same integer multiples of the ω_c. When $\Delta\omega$ is at zero, the model and observed spectra are not similar at all. The periodic phase entrainment behavior may be too

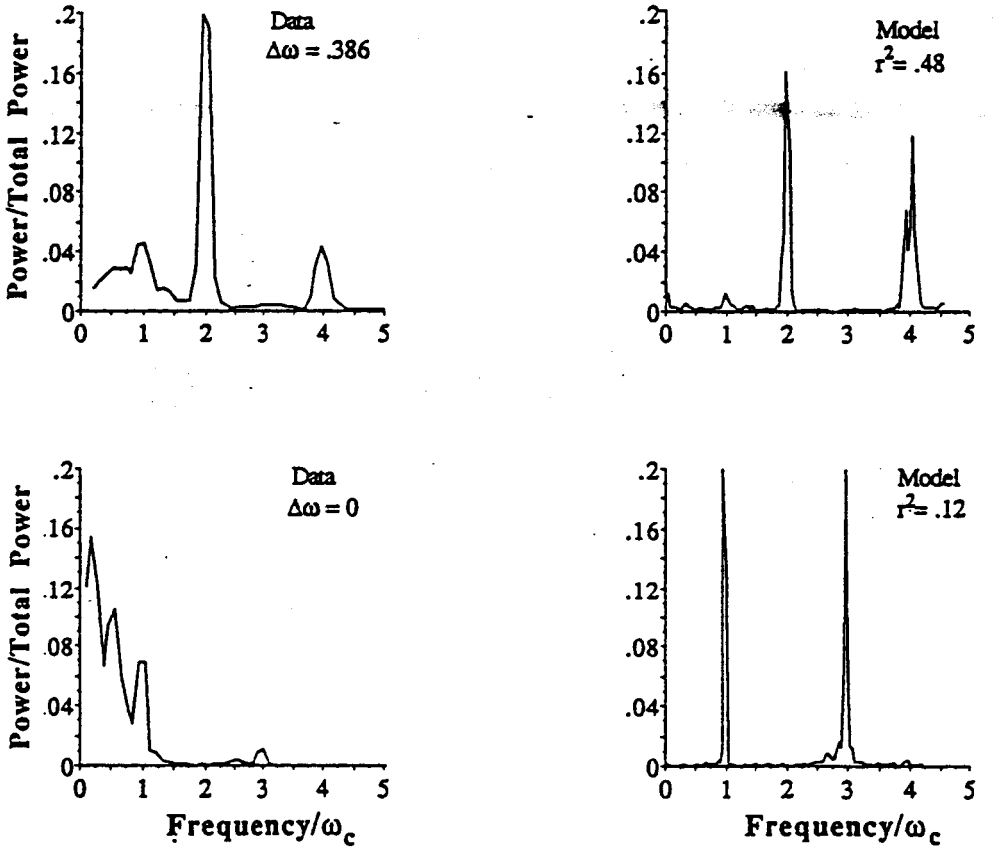

Figure 13. A comparison spectra of two representative trials, one with $\Delta\omega = .386$ (upper left panel) and one with $\Delta\omega = 0$ (lower left panel), and the spectra of the phase entrainment model fit (Equation 14) of these trials that was found through a stepwise regression (upper right and lower right panels).

small in low $\Delta\omega$ conditions to be reliably modeled. Alternatively, increasing the complexity of the coupling terms in Equation 8 may not be the correct way to model the behavior of $\dot{\Phi}$. The second hypothesis, that the difference in the oscillatory dynamics of the individual rhythmic units that is causing the phase entrainment, is currently being tested (Beek, Schmidt, Morris, Sim, & Turvey, 1991), and which of the two possible modifications of the dynamical model is best will be explored in future research.

The fit of the revised model of relative phase behavior (Equation 14) to the phase entrainment data ($\dot{\Phi}$ suggests that additional control processes are recruited as the scaling of the two control parameters $\Delta\omega$ and ω_c brings the movement control structure into regions of its state space that are increasingly less stable. The solution to maintaining the coordination is to change the control dynamic from a regime which has a point attractor, phase locking, and $\dot{\Phi}$ near 0 to one that has periodic components, phase entrainment, and relatively large values of $\dot{\Phi}$. This remedy would have the effect of keeping the control structure stable enough so that the coordination can continue to be maintained in spite of the demands of the task.

But just what these control structures amount to is still at issue. Perhaps, as has been previously suggested, because more difficult movements need increased perceptual feedback, the additional control processes are used to obtain additional perceptual information about the movements (Schmidt et al., 1991). This hypothesis can be tested by manipulating the perceptual information available and determining how the phase entrainment behavior is affected. With limited information available the coordination at extreme values of $\Delta\omega$ and ω_c should not be able to be maintained. It is planned to investigate these ideas in the visual coordination of rhythmic movements between two individuals. Interestingly, the between person adaptations of rhythmic coordination paradigms in the present article yield nearly identical patterning of relative phase with manipulation of the control parameters $\Delta\omega$ and ω_c (Schmidt et al., 1990). However, in the between person paradigm, one has the added flexibility to manipulate the availability of visual information by means of an occlusion methodology. This methodology will allow the determination of whether more perceptual tuning occurs as the $\Delta\omega$ and ω_c are scaled into their extreme ranges and whether perceptual control structures underlie the peaks of the Φ spectrum.

References

Beek, P. J. (1989). Juggling dynamics. Amsterdam: Free University Press.

Beek, P. J., Schmidt, R. C., Morris, A. W., Sim, M-Y., & Turvey, M. T. (1991 October). *Determining stiffness and friction terms in rhythmic movements.* Poster presentation at the 18th Meeting of the International Society for Ecological Psychology, Hartford, CT.

Beek, P. J., Turvey, M. T., & Schmidt, R. C. (1992). Autonomous and nonautonomous dynamics in coordinated rhythmic movements. *Ecological Psychology, 4,* 65–95.

Bingham, G. P., Schmidt, R. C., Turvey, M. T., & Rosenblum, L. D. (1991). Task dynamics and resource dynamics in the assembly of a coordinated rhythmic activity. *Journal of Experimental Psychology: Human Perception and Performance, 17,* 359–381.

Gilmore, R. (1981). *Catastrophe theory for scientists and engineers.* New York: Wiley.

Goldberger, A. L., Bhargava, V., West, B. J., & Mandell, A. J. (1985). On a mechanism of cardiac electrical stability: The fractal hypothesis. *Biophysics Journal, 48,* 525–528.

Goldberger, A. L., Kobalter, K., & Bhargava, V. (1986). 1/*f*-like scaling in normal neutrophil dynamics: Implications for hematologic monitoring. *IEEE Transactions on Biomedical Engineering, 33,* 874–876.

Haken, H. (1983). *Synergetics: An introduction.* Heidelberg, Federal Republic of Germany: Springer-Verlag.

Haken, H., Kelso, J. A. S., & Bunz, H. (1985). A theoretical model of phase transitions in human hand movements. *Biological Cybernetics, 51,* 347–356.

Iberall, A. S. (1977). A field and circuit thermodynamics for integrative physiology: I. Introduction to the general notions. *American Journal of Physiology, 233,* R171–R180.

Iberall, A. S. (1978). A field and circuit thermodynamics for integrative physiology: III. Keeping the books—A general experimental method. *American Journal of Physiology, 234,* R85–R97.

Keith, W. L., & Rand, R. H. (1984). 1:1 and 2:1 phase entrainment in a system of two coupled limit cycle oscillators. *Journal of Mathematical Biology, 20,* 133–152.

Kelso, J. A. S. (1984). Phase transitions and critical behavior in human bimanual coordination. *American Journal of Physiology: Regulatory, Integrative and Comparative, 246,* R1000–R1004.

Kelso, J. A. S. (1989). Phase transitions: Foundations of behavior. In H. Haken (Ed.), *Synergetics of cognition* (pp. 249–268). Berlin: Springer.

Kelso, J. A. S., & Kay, B. A. (1987). Information and control: A macroscopic analysis of perception-action coupling. In H. Heuer & A. F. Sanders (Eds.), *Tutorials in perception and action* (pp. 3–32). Amsterdam: North-Holland.

Kelso, J. A. S., Scholz, J. P., & Schöner, G. (1986). Nonequilibrium phase transitions in coordinated biological motion: Critical fluctuations. *Physics Letters, 118,* 279–284.

Koboyashi, M., & Musha, T. (1982). 1/*f* fluctuation of heartbeat period. *IEEE Transaction on Biomedical Engineering, 29,* 456–457.

Kopell, N. (1988). Toward a theory of modelling central pattern generators. In A. H. Cohen, S. Rossignol, & S. Grillner (Eds.), *Neural control of rhythmic movements in vertebrates* (pp. 369–413). New York: Wiley.

Kugler, P. N. (1990). *Physics of complex systems: Atomisms and continua.* Colloquium at the Center for the Ecological Study of Perception and Action, University of Connecticut, Storrs, CT.

Kugler, P. N., Kelso, J. A. S., & Turvey, M. T. (1980). On the concept of coordinating structures as dissipating structures: I. Theoretical lines of convergence. In G. E. Stelmach & J. Requin (Eds.), *Tutorials in motor behavior* (pp. 3–47). Amsterdam: North-Holland.

Kugler, P. N., & Turvey, M. T. (1987). *Information, natural law and the self-assembly of rhythmic movement.* Hillsdale, NJ: Erlbaum.

Musha, T., Katsurai, K., & Teramachi, Y. (1985). Fluctuation of human tapping intervals. *IEEE Transactions on Biomedical Engineering, 32,* 578–581.

Partridge, L. D. (1966). Signal-handling characteristics of load-moving skeletal muscle. *American Journal of Physiology, 210,* 1178–1191.

Partridge, L. D. (1967). Intrinsic feedback factors producing inertial compensation in muscle. *Biophysics Journal, 7,* 853–863.

Press, W. H., Flannery, B. P., Teukolsky, S. A., & Vetterling, W. T.

(1988). *Numerical recipes in C: The art of scientific computing.* Cambridge, England: Cambridge University Press.

Rand, R. H., Cohen, A. H., & Holmes, P. J. (1988). Systems of coupled oscillators as models of central pattern generators. In A. H. Cohen, S. Rossignol, & S. Grillner (Eds.), *Neural control of rhythmic movements in vertebrates.* New York: Wiley.

Rosenblum, L. D., & Turvey, M. T. (1988). Maintenance tendency in coordinated rhythmic movements: Relative fluctuations and phase. *Neuroscience, 27,* 289–300.

Schmidt, R. C., Beek, P. J., Treffner, P. J., & Turvey, M. T. (1991). Dynamical substructure of coordinated rhythmic movements. *Journal of Experimental Psychology: Human Perception and Performance, 17,* 635–651.

Schmidt, R. C., Carello, C., & Turvey, M. T. (1990). Phase transitions and critical fluctuations in the visual coordination of rhythmic movements between people. *Journal of Experimental Psychology: Human Perception and Performance, 16,* 227–247.

Scholz, J. P., Kelso, J. A. S., & Schöner, G. (1987). Nonequilibrium phase transitions in coordinated biological motion: Critical slowing down and switching time. *Physics Letters, 123,* 390–394.

Schöner, G., Haken, H., & Kelso, J. A. S. (1986). A stochastic theory of phase transitions in human hand movement. *Biological Cybernetics, 53,* 247–257.

Stein, P. S. G. (1973). The relationship of interlimb phase to oscillator activity gradients in crayfish. In R. B. Stein, K. G. Pearson, R. S. Smith, & J. B. Redford (Eds.), *Control of posture and locomotion* (pp. 621–623). New York: Plenum Press.

Stein, P. S. G. (1974). The neural control of interappendage phase during locomotion. *American Zoologist, 14,* 1003–1016.

Sternad, D., Turvey, M. T., and Schmidt, R. C. (1992). Average phase difference theory and 1:1 phase entrainment in interlimb coordination. *Biological Cybernetics, 67,* 223–231.

Turvey, M. T., Rosenblum, L. D., Schmidt, R. C., & Kugler, P. N. (1986). Fluctuations and phase symmetry in coordinated rhythmic movements. *Journal of Experimental Psychology: Human Perception and Performance, 12,* 564–583.

Turvey, M. T., Schmidt, R. C., Rosenblum, L. D., & Kugler, P. N. (1988). On the time allometry of coordinated rhythmic movements. *Journal of Theoretical Biology, 130,* 285–325.

von Holst, E. (1973). Relative coordination as a phenomenon and as a method of analysis of central nervous system function. In R. Martin (Ed. & Trans.), *The collected papers of Erich von Holst: Vol. 1. The behavioral physiology of animal and man* (pp. 33–135). Coral Gables, FL: University of Miami Press. (Original work published 1939)

West, B. J., & Shlesinger, M. F. (1990). The noise in natural phenomena. *American Scientist, 78,* 40–45.

Zanone, P. G., & Kelso, J. A. S. (1992). The evolution of behavioral attractors with learning: Nonequilibrium phase transitions. *Journal of Experimental Psychology: Human Perception and Performance, 18,* 403–421.

Received November 14, 1991
Revision received May 11, 1992
Accepted May 13, 1992 ■